



Early View

Original article

SPLUNC1 Degradation by the Cystic Fibrosis Mucosal Environment Drives Airway Surface Liquid Dehydration

Megan J. Webster, Boris Reidel, Chong D. Tan, Arunava Ghosh, Neil E. Alexis, Scott H. Donaldson, Mehmet Kesimer, Carla M.P. Ribeiro, Robert Tarran

Please cite this article as: Webster MJ, Reidel B, Tan CD, *et al.* SPLUNC1 Degradation by the Cystic Fibrosis Mucosal Environment Drives Airway Surface Liquid Dehydration. *Eur Respir J* 2018; in press (<https://doi.org/10.1183/13993003.00668-2018>).

This manuscript has recently been accepted for publication in the *European Respiratory Journal*. It is published here in its accepted form prior to copyediting and typesetting by our production team. After these production processes are complete and the authors have approved the resulting proofs, the article will move to the latest issue of the ERJ online.

Copyright ©ERS 2018

SPLUNC1 Degradation by the Cystic Fibrosis Mucosal Environment Drives Airway Surface Liquid Dehydration

**Megan J. Webster¹, Boris Reidel¹, Chong D. Tan¹, Arunava
Ghosh¹, Neil E. Alexis², Scott H. Donaldson^{1,4}, Mehmet Kesimer¹,
Carla M.P. Ribeiro^{1,3} and Robert Tarran^{1,3}**

¹Marsico Lung Institute, ²Center for Asthma and Lung Biology, ³Department of Cell Biology & Physiology, ⁴Division of Pulmonary and Critical Care Medicine, The University of North Carolina, Chapel Hill, NC, 27599,

Running Title: SPLUNC1 & CF Sputum

Correspondence to: Robert Tarran
7102 Marsico Hall,
125 Mason Farm Road
University of North Carolina
Chapel Hill, NC, 27599
Email: robert_tarran@med.unc.edu
Contact: 919-966-7052

07.06.18

Conflicts of Interest

RT is founder of and has equity in Spyryx Biosciences. CMPR is founder of and has equity in Irex Pharma. No other conflicts exist.

Abstract

Mutations in the cystic fibrosis transmembrane regulator (*CFTR*) gene, which lead to diminished transepithelial anion transport, cause the multi-organ disease cystic fibrosis (CF). CF lungs are characterised by airway surface liquid (ASL) dehydration, chronic infection/inflammation and neutrophilia. Dysfunctional CFTR may up-regulate the epithelial Na⁺ channel (ENaC), further exacerbating dehydration. We previously demonstrated that the short palate lung and nasal epithelial clone 1 (SPLUNC1) negatively regulates ENaC in normal airway epithelia. Here, we used pulmonary tissue samples, sputum and human bronchial epithelial cultures (HBECs) to determine whether SPLUNC1 could regulate ENaC in a CF-like environment. We found reduced endogenous SPLUNC1 in CF secretions, and rapid degradation of recombinant SPLUNC1 (rSPLUNC1) by CF secretions. Interestingly, normal sputum, containing SPLUNC1 and SPLUNC1-derived peptides, inhibited ENaC in both normal and CF HBECs. Conversely, CF sputum activated ENaC and rSPLUNC1 could not reverse this phenomenon. Additionally, we observed upregulation of ENaC protein levels in human CF bronchi. Unlike SPLUNC1, the novel SPLUNC1-derived peptide, SPX-101, resisted protease degradation, bound apically to HBECs, inhibited ENaC and prevented ASL dehydration following extended pre-incubation with CF sputum. Our data indicate CF mucosal secretions drive ASL hyperabsorption and protease-resistant peptides, like SPX-101, can reverse this effect to re-hydrate CF ASL.

Introduction

Cystic fibrosis (CF) is a genetic, multi-organ disease caused by mutations in the CF transmembrane conductance regulator (*CFTR*) gene that result in defective transepithelial anion transport (1). In the airways, ENaC is the rate-limiting step that governs transepithelial Na⁺ absorption (2). The absence of CFTR leads to increased ENaC activity and Na⁺ hyperabsorption, which in combination with anion hyposalivation causes ASL dehydration reducing mucociliary clearance (3-5). Together, these changes are predicted to cause the accumulation of dehydrated intraluminal mucus plugs that serve as a nidus for subsequent bacterial infections. A failure to resolve these infections causes chronic inflammation/neutrophilia and elevated lung luminal protease levels. These proteases, including neutrophil elastase (NE) and cathepsins B, S, L, then cause bronchiectasis and ultimately destroy the lung (6, 7). Indeed, a correlation between NE activity and CF lung disease severity has recently been reported (8).

Short palate lung and nasal epithelial clone 1 (SPLUNC1) is a multi-functional 25 kDa innate defence protein that is secreted into the airway surface liquid (ASL) (9-12). SPLUNC1 is an allosteric regulator that binds extracellularly causing a conformational change to ENaC. This binding event is followed by NEDD4.2-dependent ubiquitination of α ENaC and subsequent internalisation of the channel, which serves to reduce Na⁺ and ASL absorption (11-13). Resolution of the SPLUNC1's crystal structure has allowed assignment of its functions to distinct regions. For example, the N-terminal 'S18' region inhibits the epithelial Na⁺ channel (ENaC) to modulate ASL volume (11, 12).

Interactions between CFTR and ENaC have been reported in heterologous expression systems (4, 14, 15). However, the nature of these interactions and the underlying mechanism of Na⁺ hyperabsorption are unknown. As such, the role of ENaC in CF lung pathophysiology remains

controversial (16, 17). SPLUNC1 inhibits ENaC in normal ASL. However, due to a series of pH-sensitive salt bridges, SPLUNC1 fails to function in the moderately acidic CF ASL (~pH 6.5)(11). Thus, under thin film conditions where native ASL has accumulated, SPLUNC1 can spontaneously inhibit ENaC in normal but not CF epithelia. Since they lack the pH-sensitive salt bridges, peptides of SPLUNC1's ENaC inhibitory domain are pH-independent and inhibit ENaC in CF-affected epithelia (12). For example, a SPLUNC1-derived peptide, SPX-101, is currently undergoing clinical trials for the treatment of CF lung disease (18). We have previously focused on the initiating events in CF (5, 11). However, given the high levels of neutrophilia and protease activity within CF airways, we postulated that endogenous SPLUNC1 was susceptible to a non-pH related degradation in CF lungs, which if it occurred within the S18 region, would prevent ENaC inhibition. Thus, using patient-derived samples, we tested the hypotheses that (i) SPLUNC1 is degraded in CF airways, leading to increased ENaC activity and (ii) that SPX-101 could overcome this deficiency to induce ENaC inhibition and rehydrate CF ASL.

Methods

A detailed description of Methods used is provided in the online supplement.

Normal/CF sputum and supernatant of mucopurulent material (SMM). Induced and spontaneous sputum samples were obtained as described (9). SMM was harvested from the airways of excised human CF lungs as described (19). Donor demographics are shown in supplementary tables 1, 2 and 3.

Proteins and peptides. SPLUNC1 was expressed and purified as described previously (11). SPX-101 (aaLPIPLDQTaa) was prepared by solid-state Fmoc synthesis as described (18).

Western blot. Endogenous NE and SPLUNC1 protein levels were determined using neat sputum samples from 18 donors. For degradation experiments, PBS, NE, normal or CF sputa (pooled from N = 6 donors/group) and SMM (pooled from N = 3 donors) were co-incubated with 10 μ M rSPLUNC1 at 37°C. Where applicable, inhibitors were pre-incubated with sputa for one hour prior to rSPLUNC1 incubation.

Neutrophil elastase activity assay. NE activity levels were determined using the NE sensitive peptide Suc-Ala-Ala-Ala-MCA as described in the supplementary material.

ENaC and Na⁺/K⁺-ATPase expression in human bronchi. Human lungs were obtained as described above, donor demographics are shown in table 3. Bronchi were dissected from the underlying tissue; CF bronchi were selected from relatively disease-free regions. Tissues were rinsed using a lactated Ringers solution and proteins extracted using lysis buffer containing NP40 (20).

Determination of rSPLUNC1 and SPX-101 cleavage by mass spectrometry. 10 μ M rSPLUNC1 and SPX-101 were incubated with pooled normal or CF sputa (N = 6 donors/group). Samples were snap frozen at -80°C and prepared by filter-aided sample preparation for proteomics

(21). Solubilized peptide material was injected for label-free quantitative proteomic analysis utilizing a Q Exactive (Thermo Scientific) mass spectrometer coupled to an UltiMate 3000 (Thermo Scientific) nanoHPLC system, and data acquisition was performed as described (22).

Human bronchial epithelial cell culture. Cells were harvested from human lungs deemed unsuitable for transplantation (non-CF donors) or post-transplantation (CF donors) as per UNC protocol #03-1396 and cultured as described on permeable supports and maintained at air-liquid interface in a modified bronchial epithelial growth medium (20). Cells were studied 21-28 days after seeding.

ASL height measurements. 30 μ M rSPLUNC1 or SPX-101 were co-incubated with PBS or pooled normal/CF sputa (N = 6 donors/group) overnight at 37°C \pm sivelestat before addition to HBEC mucosal surfaces and ASL heights were measured as described previously (11).

Binding of SPLUNC1 and SPX-101 to HBECs. Cells were exposed apically to either amine-reactive Dylight-633 rSPLUNC1 or 5-TAMRA - SPX-101 pre-incubated with PBS, normal or CF pooled sputa. Cells were counterstained using Calcein-AM and imaged using a Leica SP8 confocal microscope.

Transepithelial Potential Difference. A single-barreled transepithelial potential difference (V_t)-sensing microelectrode was positioned in the ASL by a micromanipulator and used in conjunction with a macroelectrode in the serosal solution to measure V_t using a voltmeter (World Precision Instruments) as described (11, 23)

Statistics. Normally distributed data were analysed using ANOVA followed by the Tukey Test or Student's t-test. Non-parametric equivalents (Mann-Whitney U-test; Kruskal Wallis Test with Dunn's Multiple Comparisons Test) were used when data were not normally distributed. For SPLUNC1 degradation over time, curves were fit with single exponentials and analyzed using the

Extra Sum of Squares F Test. Data analysis was performed using GraphPad Prism 7.0. Significance values are denoted as follows; * $P < 0.05$, ** $P < 0.01$, *** $P < 0.001$ and **** $P < 0.0001$.

Results

SPLUNC1 protein levels are decreased in CF sputum. Consistent with previous studies, we detected SPLUNC1 levels by Western blot analysis in normal sputum samples (9, 24). However, we detected a significant reduction in endogenous SPLUNC1 protein levels in CF sputum (figure 1). Since NE can degrade SPLUNC1 (24), we next determined NE protein levels. In agreement with previous studies (25), we found increased NE levels in CF samples (figure 1a and b). We next co-incubated recombinant SPLUNC1 (rSPLUNC1) with pooled sputa from normal and CF donors. Full-length rSPLUNC1 was exponentially degraded by CF sputum ($t_{1/2} = 26$ min), but remained stable following incubation with normal sputum (figure 2a and b). Since CF lung disease increases the ASL protein content, we co-incubated rSPLUNC1 with volume-adjusted normal and CF sputa to test for rSPLUNC1 degradation independently of protein concentrations. rSPLUNC1 levels were significantly reduced in the presence of CF sputum only (figure 2c and d). To confirm that the degradation of SPLUNC1 was protein-mediated, sputum samples were incubated with normal/CF sputum at 4°C or in the presence of heat denatured normal and CF sputum (95°C/ β -mercaptoethanol). Both of these maneuvers attenuated rSPLUNC1 degradation in CF sputum (Figure S1a and b). ~~To confirm that SPLUNC1 degradation was protein-mediated, samples were heat denatured in the presence of β -mercaptoethanol. rSPLUNC1 degradation was attenuated in heat denatured CF sputum (supplementary figure S1a and b).~~ Since collection methods differed for normal and CF sputa (i.e. induced vs. spontaneous collection respectively), we confirmed that rSPLUNC1 stability was unaffected by the collection method and we found no difference in SPLUNC1 stability in spontaneous vs. induced sputum (supplementary figure S2).

NE in CF sputum is partially responsible for SPLUNC1 degradation. We co-incubated rSPLUNC1 and CF sputum with inhibitors of several proteases, their respective inhibitors, and an EDTA free protease inhibitor cocktail (PIC), used to inhibit multiple proteases (19). Only sivelestat and 10x PIC significantly attenuated rSPLUNC1 degradation (figure 3a and b). In contrast, all other inhibitors failed to attenuate rSPLUNC1 degradation (figure 3a and b). Since NE was elevated in CF sputum, and SPLUNC1's degradation was sivelestat-sensitive, we co-incubated rSPLUNC1 with NE, which degraded rSPLUNC1 in a concentration dependent manner (figure 3c and d). Due to the potential importance of these findings, we exposed rSPLUNC1 to normal/CF sputa in the presence of protease inhibitors for extended times. Surprisingly, sivelestat was unable to prevent rSPLUNC1 degradation after extended incubation periods (figure 4a and b).

To confirm the translation of high NE protein levels into elevated NE activity, we added a NE-sensitive substrate to sputum \pm sivelestat, and measured formation of the fluorescent product, AMC, which was significantly elevated after exposure to CF but not normal sputum (figure 4c). Sivelestat was unable to reduce AMC formation following 12 hours of exposure to CF sputum (figure 4d) and failed to recover SPLUNC1's ability to regulate ASL height (supplementary figure 3a and b). Additionally, we tested whether cathepsins B, K, S and L were active in CF sputum. Using protease-specific fluorogenic substrates, we observed significantly greater cathepsin B, cathepsin K and cathepsin S/L activity in CF sputum (figure S3a, b). We also measured MMP-2/9 activity which was significantly elevated in CF sputum. Since the inhibitors of these enzymes failed to attenuate rSPLUNC1 degradation, we conclude that while a number of proteases are functionally active in CF sputum, that NE is predominantly responsible for rSPLUNC1 degradation.

Up-regulation of α -, β -, and γ - ENaC and Na^+/K^+ ATPase $\alpha 1$ protein expression in CF bronchi indicates increased ENaC activity. SPLUNC1 was undetectable in SMM collected

from excised CF lungs (figure 5a). Similarly, co-incubation of SMM and rSPLUNC1 resulted in a rapid diminution of rSPLUNC1 (figure 5b and c). Since SPLUNC1 affects ENaC proteostasis (13), we measured ENaC levels. Bronchi were collected from non-CF and relatively disease-free areas of CF lungs and we measured protein levels by Western blot (11). We observed a significant increase all ENaC subunits in CF bronchi (figure 5d and e). α and γ ENaC must be proteolytically cleaved before ENaC can conduct Na^+ (26). Interestingly, we detected significant increases in cleaved ENaC subunits in CF bronchi, suggesting that ENaC activity is upregulated (figure 5d and e). Consistent with increased ENaC levels, the the Na^+/K^+ ATPase $\alpha 1$ subunit was also increased in CF bronchi (figure 5d and e).

CF sputum cleaves the ENaC inhibitory domain of SPLUNC1. NE predominantly cleaves valine and alanine residues. Indeed, co-incubation of rSPLUNC1 with CF but not normal sputum generated elastase-specific peptides. As a control, we performed a tryptic digest and here, peptides were detected regardless of genotype (figure 6a). Coverage analysis revealed valine-specific cleavage of SPLUNC1's S18 region (GGLPVPLDQTLPLNVPA) and the formation of PLDQTLPLNV, which is likely unable to regulate ENaC (figure 6b). We recently developed a novel, NE-resistant, SPLUNC1 derived peptide called SPX-101 (18). The ENaC interacting region of the SPX-101 peptide remained intact following exposure to CF sputum (figure 6b). To determine if rSPLUNC1 and SPX-101 remained active in the presence of CF sputum, we co-incubated PBS or sputum with rSPLUNC1 or SPX-101 overnight and added this apically to HBECs established from normal donors. rSPLUNC1 and SPX-101 increased ASL height in the presence of PBS and normal sputum (figure 6c and d). Consistent with mass spectrometry data, only SPX-101, was capable of regulating ASL height in the presence of CF sputum (figure 6c and d).

CF sputum prevents SPLUNC1 binding and elevates ENaC activity. Since ENaC is apically expressed, SPLUNC1 must also bind apically as part of the inhibition process (13). We therefore co-incubated fluorescently labelled rSPLUNC1 and SPX-101 with PBS or sputum, before apical addition to HBECs. We observed apical binding of Dylight633-rSPLUNC1 and 5-TAMRA-SPX-101 in both PBS and normal sputa-treated HBECs (figure 7a). However, after exposure to CF sputum, SPX-101, but not SPLUNC1 was able to bind apically (figure 7a). Furthermore, SPX-101 but not SPLUNC1, remained functionally active and internalised α ENaC-GFP following exposure to NE, (supplementary figure S4).

We next determined whether SPLUNC1 degradation by CF secretions contributed to ENaC hyperactivity. We have previously reported increases in ENaC activity in primary CF HBECs (23). However, passaged HBECs do not display this phenomenon. So, to start with similar transepithelial voltages (V_t s), we exposed passaged normal and CF HBECs to normal or CF sputum, or PBS (control) and measured the resultant amiloride-sensitive V_t as a marker of ENaC activity. Baseline amiloride-sensitive V_t 's were not significantly different between normal and CF HBECs (figure 7b and c). However, addition of normal sputum reduced V_t whilst CF sputum significantly elevated V_t , independently of HBEC genotype. Addition of rSPLUNC1 in PBS significantly reduced V_t in normal but not CF HBECs, consistent with our previous findings that SPLUNC1 cannot function in CF HBECs (11). rSPLUNC1 was without further effect on the already reduced V_t in HBECs exposed to normal sputum, suggesting that endogenous S18-like peptides were present in sufficient quantities to inhibit ENaC as described (12). Normal but not CF sputum was able to significantly decrease the CF V_t (Fig 7C), suggesting that spontaneously-produced, bioactive peptides are present in normal but not CF sputum. To further examine this effect, we passed normal sputum through a size exclusion column to remove peptides/proteins ≥ 10

kDa. We then added this filtrate to normal HBECs and measured ASL height 6 h later. Indeed, this filtrate significantly increased ASL height and addition of 30 μ M rSPLUNC1 to filtrate was without further effect (Fig S5). Consistent with our previous observation that full length SPLUNC1 is inactive in CF airways, rSPLUNC1 failed to reduced amiloride-sensitive V_t in the presence of CF sputum. SPX-101 was able to significantly inhibit the amiloride-sensitive V_t in both normal and CF HBECs after exposure to either PBS or CF sputum (figure 7b and c).

Discussion

The lung mucosal environment contains ~1,000 proteins, of which ~5% are proteases and their inhibitors (27). Under normal conditions, anti-proteases prevent excessive NE activity in the airways (28). In general, SPLUNC1 was relatively stable in normal sputum (figure 1), although in some cases, we did observe some degradation (e.g. Fig S2). However, the degradation product was close size to full length SPLUNC1 (>20 kDa) and was similar in size to a SPLUNC1-degradation product that we had previously observed after exposing SPLUNC1 to trypsin (29). Thus, we speculate that serine proteases present in normal ASL/sputum may post-translationally affect SPLUNC1. However, chronic neutrophilia in the CF lung lumen significantly increases free NE levels (8, 28, 30). Similarly, we found significantly higher NE protein levels and activity in CF sputum compared with sputum from normal healthy donors (figure 1). We also observed that SPLUNC1 protein levels were significantly reduced in CF sputum and that rSPLUNC1 was rapidly degraded in CF sputum (figures 1, 2). To confirm that SPLUNC1 was degraded, we also performed proteomic analysis. Indeed, NE-specific SPLUNC1 coverage was markedly increased in CF sputum, indicating inflammation-induced degradation. Crucially, intact S18-like peptides that can inhibit ENaC, were absent in CF sputum. Despite being cleaved by NE, SPLUNC1 remains aggregated for several hours before dissociating (31). However, the lack of SPLUNC1 coverage in CF sputum, and the relatively short half-life of rSPLUNC1 in CF sputum, suggest that at steady state, SPLUNC1 does not exist as a functional entity in CF airway secretions.

NE inhibitors have previously been tested in CF patients, with little effect. For example, AZD9668 was tested in CF patients and had no effect on inflammation or lung function (32). Similarly, recombinant α 1 anti-trypsin also failed to affect lung inflammation (6). Similarly, our data indicated that sivelestat was only partially effective at preventing SPLUNC1 degradation in

CF sputum and this effect was lost over time. ENaC is highly promiscuous and is cleaved by multiple proteases. Thus, possible contributions to the failure of NE inhibitors in the clinic are (i) SPLUNC1 and other proteins are still degraded by CF secretions in the absence of NE and (ii) ENaC can still be activated by other proteases in the CF lung leading to persistent ASL dehydration. Thus, whilst newer broad-spectrum anti-proteases such as QUB-TL1 may be more effective at preventing ENaC cleavage (33), whether or not they are fully effective in the CF lung remains to be determined.

Our working hypothesis is that SPLUNC1 causes removal of ENaC from the plasma membrane, preventing its cleavage and activation. We have recently developed SPX-101, a size-optimized SPLUNC1 derivative that can inhibit ENaC in CF HBECs and CF-like animal models (18). Since SPX-101 is currently undergoing clinical trials for the treatment of CF, we tested whether SPX-101 was stable and efficacious in CF sputum samples. Both SPLUNC1 and SPX-101 increased ASL height after an overnight incubation in normal sputum. However, after exposure to CF sputum, SPLUNC1 was degraded and failed to regulate ASL height, while SPX-101 remained intact and active. As a control, we also incubated SPLUNC1 and SPX-101 overnight with NE and probed for α ENaC-GFP diminution, as an indicator of internalisation. While SPLUNC1 lost the ability to inhibit ENaC, SPX-101 again remained active even after prolonged exposure to NE (see online supplement).

SPLUNC1 was degraded in CF sputum from the central airways. However, by utilizing SMM, we also observed SPLUNC1 degradation in more distal regions of CF lungs. Consistent with the lack of SPLUNC1, we observed a significant increase in full-length α , β and γ ENaC subunits, suggesting that SPLUNC1 had failed to internalise ENaC. Crucially, α and/or γ ENaC must be proteolytically cleaved to be active (26, 34, 35) and we also detected significant increases

in cleaved α and γ ENaC subunits in CF airways. The basolateral Na^+/K^+ -ATPase serves to pump out Na^+ that enters the cell via ENaC in order to keep intracellular Na^+ at ~ 23 mM (36). This pump has previously been shown to be functionally upregulated in CF airways (37). Similarly, we also observed a significant increase in Na^+/K^+ -ATPase protein levels in CF airways, consistent with the increase in cleaved α and γ ENaC subunits. Welsh and colleagues have proposed that the increase in ENaC activity detected electrophysiologically is an artefact caused by amiloride-induced apical membrane hyperpolarisation (38, 39). However, our biochemical data, which demonstrate that cleaved (i.e. active) ENaC, as well as the necessary Na^+/K^+ -ATPase are upregulated in CF epithelia suggest that this is not the case.

Whilst defective ion transport is widely accepted to be the initial event in the pathogenesis of CF lung disease, the role of ENaC remains highly controversial (17). A number of studies have demonstrated increased electrical Na^+ flux and fluid changes in CF airway epithelia that were attributable to increased ENaC activity (3, 40). In contrast, others failed to find differences in CF piglets and in cultured airway epithelia (38, 39, 41). Our data revealed that rSPLUNC1 failed to bind to HBEC apical membranes after pre-incubation with CF sputum whilst N-terminally labelled SPX-101 bound equally well after exposure to normal or CF sputum. rSPLUNC1 was amine-labelled with DyLight633, suggesting that multiple residues were labelled. Thus, while it is possible that CF proteases may have removed some dye-labeled residues, we limited our SPLUNC1/CF sputum pre-incubation to 2 hours, at which point, $\sim 20\%$ of the protein should have remained.

In our microelectrode studies, we first added bumetanide in order to avoid any confounding effects of amiloride-induced Cl^- secretion in non-CF HBECs (23). SPLUNC1 lowered the amiloride-sensitive V_t in non-CF but not CF HBECs whilst SPX-101 lowered V_t regardless of

genotype. Here, the reduced bicarbonate secretion in CF HBECs contributes to the moderate acidification needed to prevent SPLUNC1 function. The requirement of functional CFTR for SPLUNC1 to inhibit ENaC is likely due to the presence of pH-sensitive salt bridges in the tertiary structure of SPLUNC1, which render it inactive below pH 7. Conversely, isolated ENaC-inhibitory peptides, such as SPX-101, lack the salt bridges and are pH-independent (11). Surprisingly, both non-CF and CF HBECs showed a significant decrease in the amiloride-sensitive V_t after being exposed to normal sputum for ~2 hours. This is likely due to the presence of endogenous S18-like ENaC inhibitory peptides (12). Indeed, after passing normal sputum through a size-exclusion column to remove proteins ≥ 10 kDa, including full length SPLUNC1 which is ~25 kDa, this filtrate was able to significantly increase ASL height. Interestingly, addition of rSPLUNC1 to the filtrate was without further effect (Fig S5), suggesting that the filtrate and SPLUNC1 have a similar target (i.e. ENaC). Thus, whilst we cannot state that SPLUNC1/S18 is the only ENaC-regulatory peptide in the ASL, our data indicate that small, ASL-regulatory peptides are present in normal sputum. In contrast, addition of CF sputum significantly elevated the amiloride-sensitive V_t in both non-CF and CF HBECs relative to normal sputum. As with the ASL height and binding experiments, SPLUNC1 was ineffective at ameliorating these effects, due to excessive degradation. However, SPX-101 remained active and could significantly reduce the amiloride-sensitive V_t . These changes are likely due to an abundance of proteases, many of which can cleave and activate ENaC, as well as a lack of functional SPLUNC1, or SPLUNC1-derived peptides in CF sputum. Taken together, these findings demonstrate that the CF mucosal environment (i.e. the ASL secretions) influences ion transport in established CF lung disease. Previous studies have demonstrated cellular interactions between CFTR and ENaC (4, 14, 15). However, our study is the

first to test the effects of CF airways secretions on ENaC activity and our data strongly indicate that the extracellular environment drives ENaC hyperactivity in CF airways.

In conclusion, we have shown that SPLUNC1 is absent or markedly reduced in CF airway secretions, which contributes to increased ENaC activity and ASL dehydration in CF HBECs. These data suggest that studying CF HBECs in the presence of CF sputum will serve as a more realistic model of CF airways and also indicate that novel therapies should be tested for efficacy in the presence of CF secretions.

Author Contributions

M. J. Webster, B. Reidel, C. D. Tan, A Ghosh and R. Tarran designed and performed research and analyzed data. N. E. Alexis, S. H. Donaldson and C. M. P. Ribeiro provided sputum and SMM samples, designed experiments and interpreted data. M. Kesimer designed experiments and analyzed data. M. J. Webster, B. Reidel and R. Tarran wrote the manuscript. All other authors edited and approved the manuscript.

Acknowledgements

We thank the UNC CF Center Tissue Cores for providing cells and tissue, Dr. Colin Bingle (University of Sheffield) for providing the SPLUNC1 construct, Dr. Debbie Baines (St. George's, University of London) for providing the α ENaC-GFP construct and Drs. Thomas Kleyman (University of Pittsburgh) and M. Jackson Stutts (UNC) for the β and γ ENaC constructs. Dr. Michael Miley and Ricard Feng (UNC) for purifying SPLUNC1. Finally, we would like to thank Dr. Brian Button (UNC) for allowing use of his equipment for this project. This study was funded by National Institutes of Health R01HL108927, P30DK065988, the UK Cystic Fibrosis Trust (INOVCF), Cystic Fibrosis Foundation R026-CR11 and TARRAN17G0.

References

1. Quinton PM. Chloride impermeability in cystic fibrosis. *Nature*. 1983;301(5899):421-22.
2. Matalon S, Bartoszewski R, and Collawn JF. Role of epithelial sodium channels in the regulation of lung fluid homeostasis. *Am J Physiol Lung Cell Mol Physiol*. 2015;309(11):L1229-38.
3. Boucher RC, Stutts MJ, Knowles MR, Cantley L, and Gatzky JT. Na⁺ transport in cystic fibrosis respiratory epithelia. Abnormal basal rate and response to adenylate cyclase activation. *J Clin Invest*. 1986;78(5):1245-52.
4. Stutts MJ, Canessa CM, Olsen JC, Hamrick M, Cohn JA, Rossier BC, et al. CFTR as a cAMP-dependent regulator of sodium channels. *Science*. 1995;269(5225):847-50.
5. Matsui H, Grubb BR, Tarran R, Randell SH, Gatzky JT, Davis CW, et al. Evidence for periciliary liquid layer depletion, not abnormal ion composition, in the pathogenesis of cystic fibrosis airways disease. *Cell*. 1998;95(7):1005-15.
6. Martin SL, Moffitt KL, McDowell A, Greenan C, Bright-Thomas RJ, Jones AM, et al. Association of airway cathepsin B and S with inflammation in cystic fibrosis. *Pediatr Pulmonol*. 2010;45(9):860-8.
7. Chalmers JD, Moffitt KL, Suarez-Cuartin G, Sibila O, Finch S, Furrie E, et al. Neutrophil Elastase Activity Is Associated with Exacerbations and Lung Function Decline in Bronchiectasis. *Am J Respir Crit Care Med*. 2017;195(10):1384-93.
8. Dittrich AS, Kühbandner I, Gehrig S, Rickert-Zacharias V, Twigg M, Wege S, et al. Elastase activity on sputum neutrophils correlates with severity of lung disease in cystic fibrosis. *European Respiratory Journal*. 2018;51(3).
9. Wu T, Huang J, Moore PJ, Little MS, Walton WG, Fellner RC, et al. Identification of BPIFA1/SPLUNC1 as an epithelium-derived smooth muscle relaxing factor. *Nat Commun*. 2017;8:14118.
10. Bartlett J, Gakhar L, Penterman J, Singh P, Mallampalli RK, Porter E, et al. PLUNC: a multifunctional surfactant of the airways. *Biochemical Society transactions*. 2011;39(4):1012-6.
11. Garland AL, Walton WG, Coakley RD, Tan CD, Gilmore RC, Hobbs CA, et al. Molecular basis for pH-dependent mucosal dehydration in cystic fibrosis airways. *Proceedings of the National Academy of Sciences*. 2013;110(40):15973-8.
12. Hobbs CA, Blanchard MG, Alijevic O, Tan CD, Kellenberger S, Bencharit S, et al. Identification of the SPLUNC1 ENaC-inhibitory domain yields novel strategies to treat sodium hyperabsorption in cystic fibrosis airway epithelial cultures. *Am J Physiol Lung Cell Mol Physiol*. 2013;305(12):L990-11001.
13. Kim CS, Ahmad S, Wu T, Walton WG, Redinbo MR, and Tarran R. SPLUNC1 is an allosteric modulator of the epithelial sodium channel. *The FASEB Journal*. 2018.
14. Schreiber R, Hopf A, Mall M, Greger R, and Kunzelmann K. The first-nucleotide binding domain of the cystic-fibrosis transmembrane conductance regulator is important for inhibition of the epithelial Na⁺ channel. *Proc Natl Acad Sci U S A*. 1999;96(9):5310-5.
15. Rubenstein RC, Lockwood SR, Lide E, Bauer R, Suaud L, and Grumbach Y. Regulation of endogenous ENaC functional expression by CFTR and $\Delta F508$ -CFTR in airway epithelial cells. *American Journal of Physiology - Lung Cellular and Molecular Physiology*. 2011;300(1):L88-L101.

16. Stoltz DA, Meyerholz DK, Pezzulo AA, Ramachandran S, Rogan MP, Davis GJ, et al. Cystic fibrosis pigs develop lung disease and exhibit defective bacterial eradication at birth. *Science translational medicine*. 2010;2(29):29ra31.
17. Stoltz DA, Meyerholz DK, and Welsh MJ. Origins of Cystic Fibrosis Lung Disease. *New England Journal of Medicine*. 2015;372(16):1574-5.
18. Scott DW, Walker MP, Sesma J, Wu B, Stuhlmiller TJ, Sabater JR, et al. SPX-101 Is a Novel Epithelial Sodium Channel-targeted Therapeutic for Cystic Fibrosis That Restores Mucus Transport. *Am J Respir Crit Care Med*. 2017;196(6):734-44.
19. Abdullah LH, Coakley R, Webster MJ, Zhu Y, Tarran R, Radicioni G, et al. Mucin Production and Hydration Responses to Mucopurulent Materials in Normal vs. CF Airway Epithelia. *Am J Respir Crit Care Med*. 2017;197(4):481-91.
20. Fulcher ML, and Randell SH. Human nasal and tracheo-bronchial respiratory epithelial cell culture. *Methods Mol Biol*. 2013;945:109-21.
21. Wisniewski JR, Zougman A, Nagaraj N, and Mann M. Universal sample preparation method for proteome analysis. *Nat Methods*. 2009;6(5):359-62.
22. Kesimer M, Cullen J, Cao R, Radicioni G, Mathews KG, Seiler G, et al. Excess Secretion of Gel-Forming Mucins and Associated Innate Defense Proteins with Defective Mucin Un-Packaging Underpin Gallbladder Mucocoele Formation in Dogs. *PLOS ONE*. 2015;10(9):e0138988.
23. Tarran R, Trout L, Donaldson SH, and Boucher RC. Soluble mediators, not cilia, determine airway surface liquid volume in normal and cystic fibrosis superficial airway epithelia. *J Gen Physiol*. 2006;127(5):591-604.
24. Jiang D, Wenzel SE, Wu Q, Bowler RP, Schnell C, and Chu HW. Human Neutrophil Elastase Degrades SPLUNC1 and Impairs Airway Epithelial Defense against Bacteria. *PLOS ONE*. 2013;8(5):e64689.
25. Sagel SD, Sontag MK, Wagener JS, Kapsner RK, Osberg I, and Accurso FJ. Induced sputum inflammatory measures correlate with lung function in children with cystic fibrosis. *The Journal of pediatrics*. 2002;141(6):811-7.
26. Caldwell RA, Boucher RC, and Stutts MJ. Neutrophil elastase activates near-silent epithelial Na⁺ channels and increases airway epithelial Na⁺ transport. *American Journal of Physiology - Lung Cellular and Molecular Physiology*. 2005;288(5):L813-L9.
27. Kesimer M, Kirkham S, Pickles RJ, Henderson AG, Alexis NE, Demaria G, et al. Tracheobronchial air-liquid interface cell culture: a model for innate mucosal defense of the upper airways? *American journal of physiology Lung cellular and molecular physiology*. 2009;296(1):L92-L100.
28. Birrer P, McElvaney NG, Rüdeberg A, Sommer CW, Liechti-Gallati S, Kraemer R, et al. Protease-antiprotease imbalance in the lungs of children with cystic fibrosis. *American Journal of Respiratory and Critical Care Medicine*. 1994;150(1):207-13.
29. Garcia-Caballero A, Rasmussen JE, Gaillard E, Watson MJ, Olsen JC, Donaldson SH, et al. SPLUNC1 regulates airway surface liquid volume by protecting ENaC from proteolytic cleavage. *Proceedings of the National Academy of Sciences*. 2009;106(27):11412-7.
30. Armstrong DS, Grimwood K, Carlin JB, Carzino R, Gutierrez JP, Hull J, et al. Lower airway inflammation in infants and young children with cystic fibrosis. *Am J Respir Crit Care Med*. 1997;156(4 Pt 1):1197-204.
31. Ahmad S, Tyrrell J, Walton WG, Tripathy A, Redinbo MR, and Tarran R. Short Palate, Lung, and Nasal Epithelial Clone 1 Has Antimicrobial and Antibiofilm Activities against

- the Burkholderia cepacia Complex. *Antimicrobial Agents and Chemotherapy*. 2016;60(10):6003-12.
32. Elborn JS, Perrett J, Forsman-Semb K, Marks-Konczalik J, Gunawardena K, and Entwistle N. Efficacy, safety and effect on biomarkers of AZD9668 in cystic fibrosis. *Eur Respir J*. 2012;40(4):969-76.
 33. Reihill JA, Walker B, Hamilton RA, Ferguson TE, Elborn JS, Stutts MJ, et al. Inhibition of Protease-Epithelial Sodium Channel Signaling Improves Mucociliary Function in Cystic Fibrosis Airways. *Am J Respir Crit Care Med*. 2016;194(6):701-10.
 34. Vallet V, Chraïbi A, Gaeggeler HP, Horisberger JD, and Rossier BC. An epithelial serine protease activates the amiloride-sensitive sodium channel. *Nature*. 1997;389(6651):607-10.
 35. Kleyman TR, Kashlan OB, and Hughey RP. Epithelial Na(+) Channel Regulation by Extracellular and Intracellular Factors. *Annual review of physiology*. 2018;80:263-81.
 36. Boucher RC. Human airway ion transport. Part one. *Am J Respir Crit Care Med*. 1994;150(1):271-81.
 37. Stutts MJ, Knowles MR, Gatzky JT, and Boucher RC. Oxygen consumption and ouabain binding sites in cystic fibrosis nasal epithelium. *Pediatr Res*. 1986;20(12):1316-20.
 38. Itani OA, Chen JH, Karp PH, Ernst S, Keshavjee S, Parekh K, et al. Human cystic fibrosis airway epithelia have reduced Cl⁻ conductance but not increased Na⁺ conductance. *Proc Natl Acad Sci U S A*. 2011;108(25):10260-5.
 39. Chen JH, Stoltz DA, Karp PH, Ernst SE, Pezzulo AA, Moninger TO, et al. Loss of anion transport without increased sodium absorption characterizes newborn porcine cystic fibrosis airway epithelia. *Cell*. 2010;143(6):911-23.
 40. Knowles M, Gatzky J, and Boucher R. Increased bioelectric potential difference across respiratory epithelia in cystic fibrosis. *N Engl J Med*. 1981;305(25):1489-95.
 41. Davies JC, Davies M, McShane D, Smith S, Chadwick S, Jaffe A, et al. Potential difference measurements in the lower airway of children with and without cystic fibrosis. *Am J Respir Crit Care Med*. 2005;171(9):1015-9.

Figures and Legends

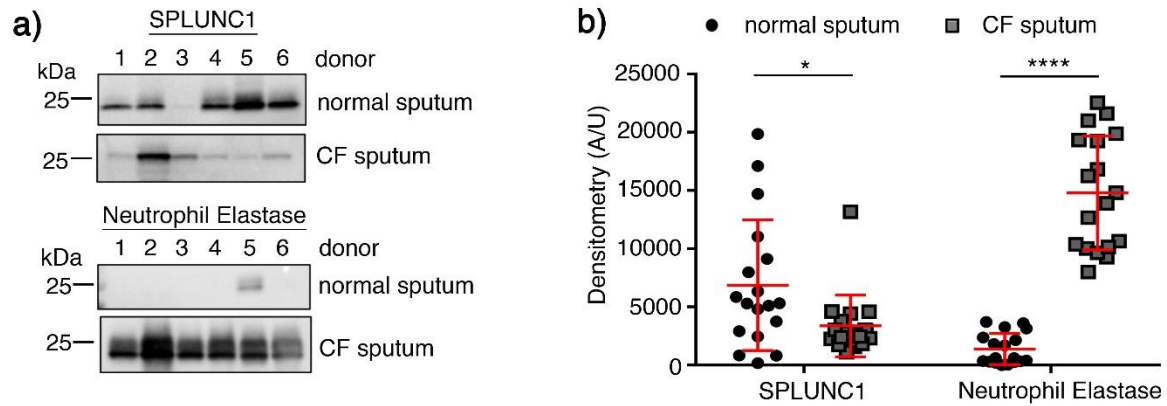


Figure 1. SPLUNC1 protein levels are significantly reduced in CF sputum. **a)** Representative western blots showing endogenous expression of SPLUNC1 and NE in normal and CF sputum samples from N = 6 donors per group. Membranes were probed for NE prior to stripping and re-probing for SPLUNC1. **b)** Densitometrical analysis of SPLUNC1 and NE protein abundance in normal and CF sputum from N = 18 donors per group. Data shown as mean \pm SD, t-test with Welch's correction, SPLUNC1 normal vs. CF sputum, * $P < 0.05$ and NE normal vs. CF sputum, **** $P < 0.0001$.

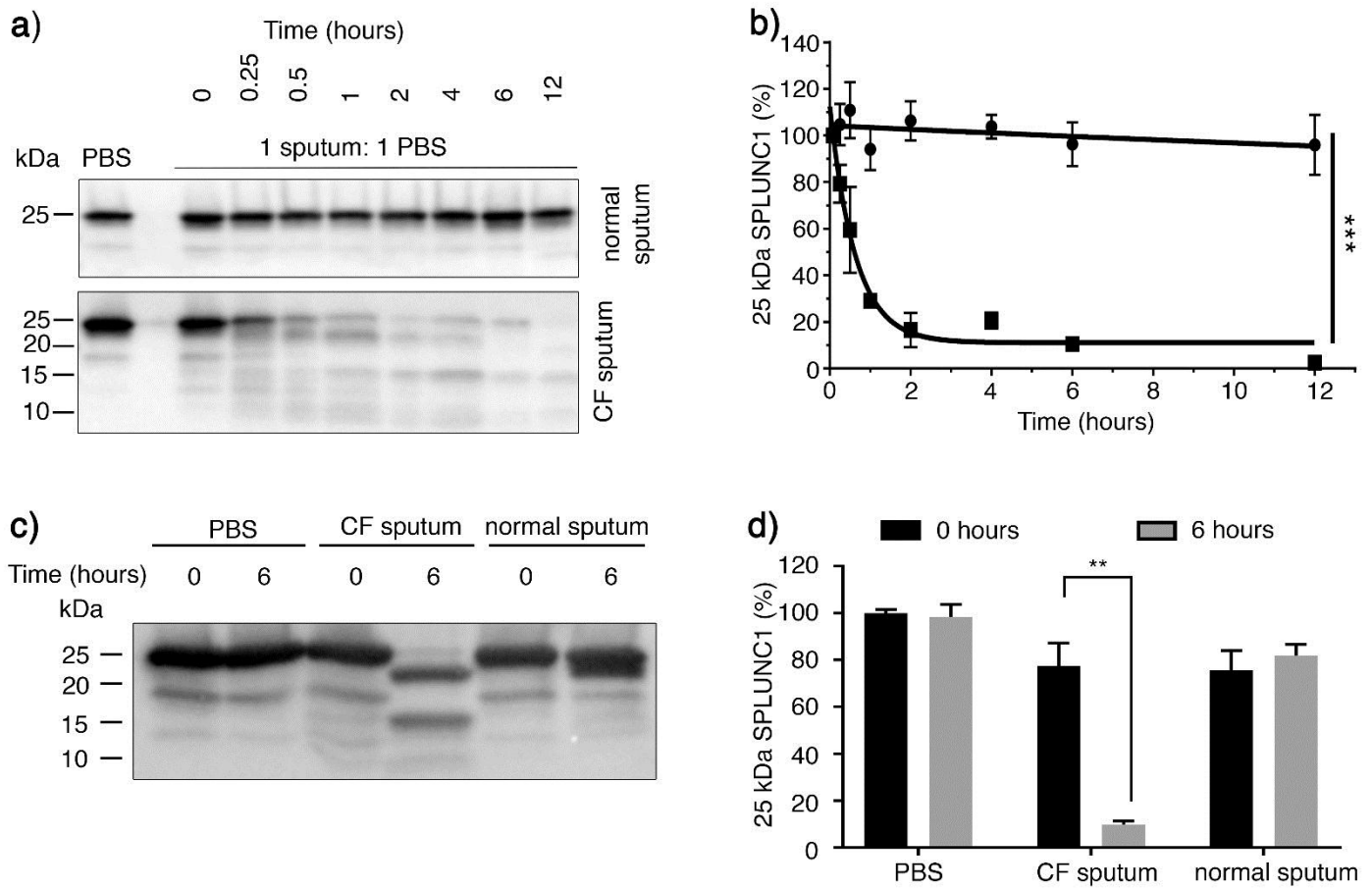


Figure 2. rSPLUNC1 is rapidly degraded in CF sputum. **a)** Representative western blots showing SPLUNC1 abundance after incubation with CF and normal sputum (pooled from N = 6 donors) at 37°C. **b)** Densitometrical analyses showing rapid degradation of rSPLUNC1. Extra sum of squares F-test, *** $P < 0.001$, rate constant (k) PBS vs. SMM rSPLUNC1 degradation. CF sputum; $t_{1/2} = \sim 26$ min, $k = 1.57$, normal sputum; $t_{1/2} = \sim 4$ hours, $k = 0.02$. Data shown mean N = 3 – 4 individual experiments \pm SD. **c)** Representative western blot showing significant degradation of 10 μ M rSPLUNC1 by CF sputum following a 6 h incubation at 37°C, with 15 μ g of total protein and **d)** associated densitometry. Data show mean N = 3-5 individual experiments \pm SEM, ** $P < 0.01$ Mann-Whitney U test.

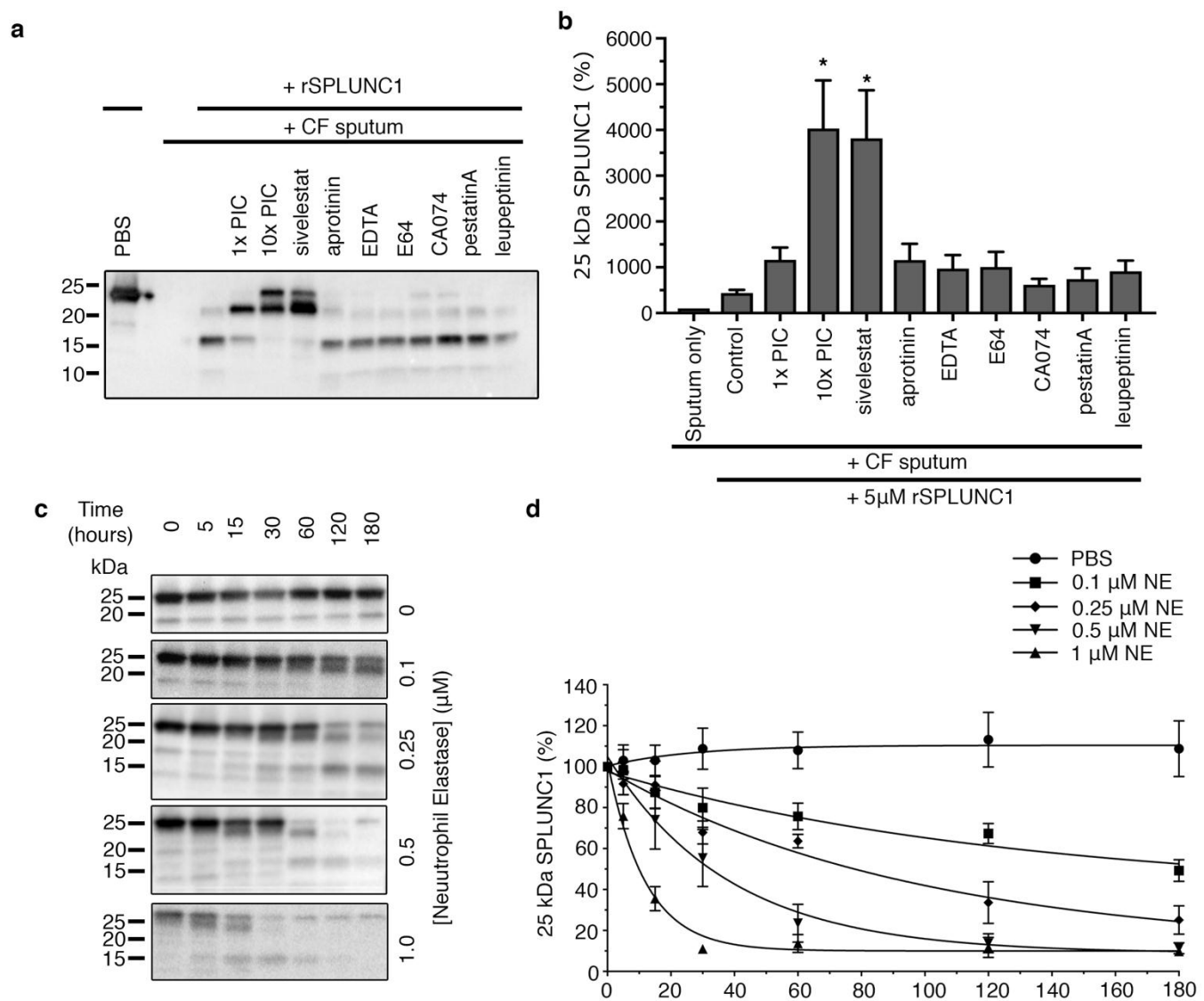


Figure 3 Sivelestat partially attenuates rSPLUNC1 degradation. **a)** representative western blot showing 25 kDa rSPLUNC1 abundance following co-incubation with 1x/ 10x protease inhibitor cocktail (PIC) or 10 μ M protease inhibitors and CF sputum (pooled from N = 6 donors) for 6 hours and associated densitometry (**b**) from N = 8 individual experiments \pm SEM, % 25 kDa SPLUNC1 expression compared with CF sputum alone. Data show significant inhibition of rSPLUNC1 degradation by 10 μ M sivelestat and 10x PIC only, * $P < 0.05$ by Kruskal–Wallis test. **c)** Representative western blots following exposure of rSPLUNC1 to NE over time and **d)** associated densitometry from N = 4 - 6 individual experiments \pm SEM. Extra sum of squares F-test, **** $P < 0.0001$, rate constant (k) different between each [NE] data set.

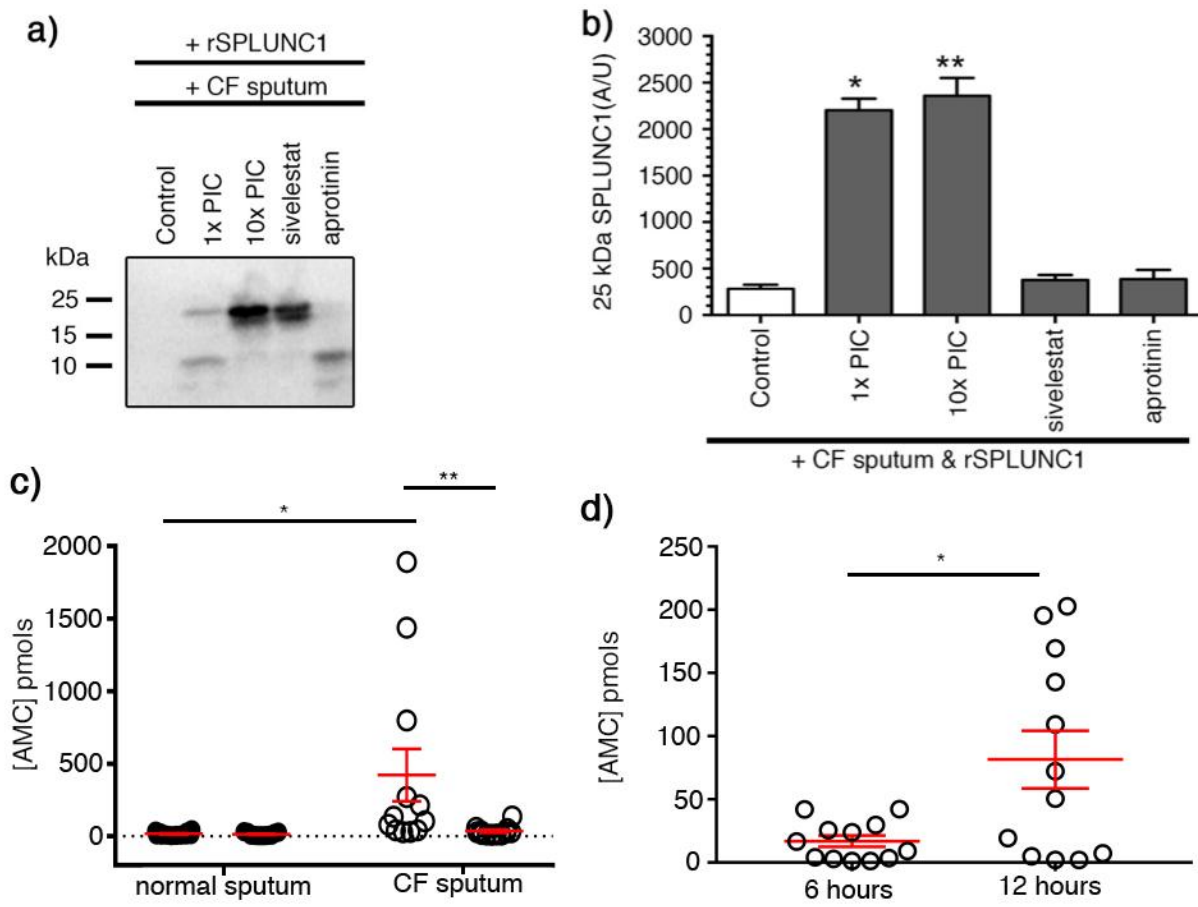


Figure 4. Sivelestat fails to prevent rSPLUNC1 degradation by CF sputum over extended periods. **a)** Representative western blot showing 25 kDa rSPLUNC1 abundance following co-incubation of 1x/ 10x protease inhibitor cocktail (PIC), 10 μ M sivelestat or 10 μ M aprotinin and CF sputum (pooled from N = 6 donors) **b)** associated densitometry from N = 3 - 4 individual experiments \pm SEM. % 25 kDa SPLUNC1 compared with CF sputum only. * $P < 0.05$, ** $P < 0.01$ by Kruskal–Wallis test. **c)** AMC formation following cleavage of 100 μ M fluorogenic substrate Suc-Ala-Ala-Ala-MCA following 6 h incubation with normal and CF sputum at 37°C \pm 10 μ M sivelestat. Data shown as mean \pm SD; normal, N = 12; CF, N = 12 individual donors, * $P < 0.05$ normal vs. CF, CF vs. CF + sivelestat ** $P < 0.01$, by Kruskal–Wallis test with Dunn’s multiple comparison. **d)** Change in AMC formation after cleavage of 100 μ M fluorogenic substrate Suc-Ala-Ala-Ala-MCA by CF sputum after 6 or 12 hours + 10 μ M sivelestat. Data shown as mean \pm SD; normal, N = 12; CF, N = 12 individual donors. * $P < 0.05$, Mann–Whitney U test.

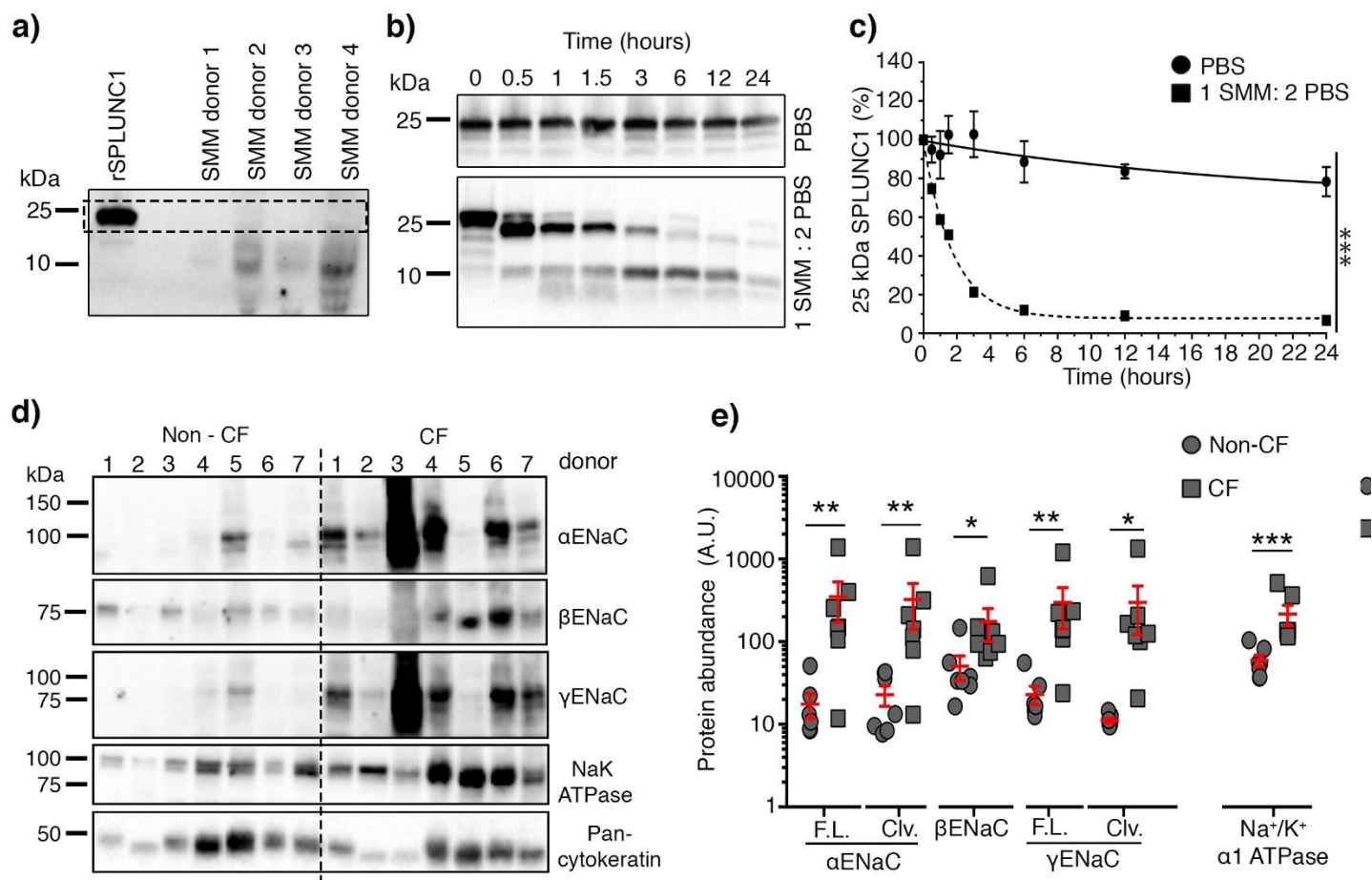


Figure 5. SPLUNC1 is degraded and α -, β -, and γ - ENaC are upregulated in CF bronchi. **a)** Western blot showing abundance of full length (F. L.) and cleaved (Clv.) α , β , and γ ENaC, as well as the Na⁺/K⁺ ATPase and pan-cytokeratin in bronchi dissected from 7 non-CF and 7 CF lungs post-mortem or post-transplant. **b)** Associated densitometry, data shown are mean \pm SD, log₁₀ transformed. Protein abundance was normalised to pan-cytokeratin expression for each individual donor. Normal vs. CF expression; * $P < 0.05$, ** $P < 0.01$ and *** $P < 0.001$, Mann Whitney U test. **c)** Western blot showing endogenous SPLUNC1 levels in SMM extracted from 4 individual CF donor lungs obtained post-transplant. **d)** Representative western blots showing 10 μ M rSPLUNC1 levels over time in PBS or SMM diluted 1:2 in PBS (SMM pooled N = 3 – 4 donors). **e)** Associated densitometry of 25 kDa SPLUNC1. Data are from N = 3 independent experiments \pm SD. Extra sum of squares F-test, *** $P < 0.001$, rate constant (k) PBS vs. SMM rSPLUNC1 degradation. PBS; $t_{1/2} = 14.6$ hours, $k = 0.05$, SMM; $t_{1/2} = 1.2$ hours, $k = 0.60$.

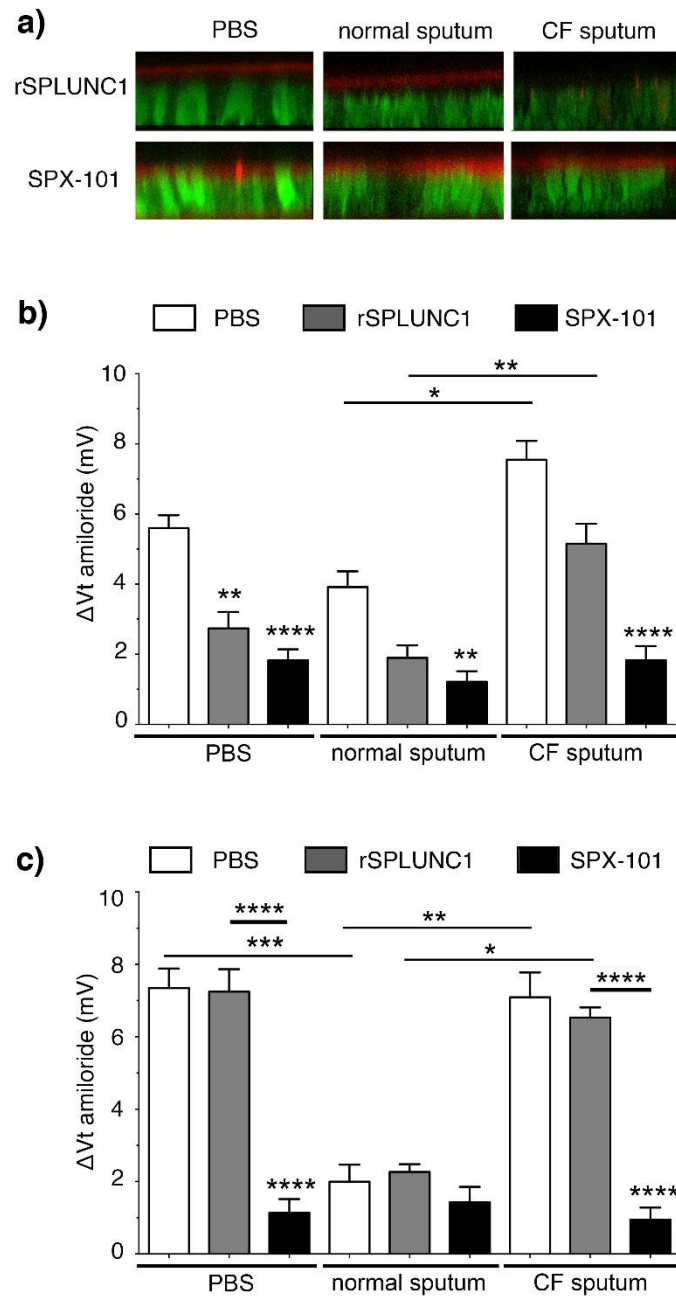


Figure 7. CF sputum prevents SPLUNC1 binding to HBEC mucosal surfaces and elevates the amiloride-sensitive V_t . **a)** Dylight633-rSPLUNC1 and TAMRA-SPX-101 were incubated with PBS, normal and CF sputum for 2 hours at 37°C and added mucosally to HBECs for an additional 2 h before imaging. XZ confocal micrographs showing apical binding of Dylight633-rSPLUNC1 and TAMRA-SPX-101 (red) to normal HBECs. HBECs were stained with calcein-AM (green). **b and c)** 30 μ M rSPLUNC1 and SPX-101 were incubated with PBS, normal or CF sputum (pooled from N = 6 donors) for 12 hours at 37°C and was added mucosally to HBECs for an additional 2 - 3 h. Voltage-sensing microelectrodes were then positioned in the ASL by micromanipulator and the amiloride-sensitive V_t was measured. N.B., all V_t measurements were performed in the presence of basolateral 10 μ M bumetanide to inhibit Cl^- secretion. Delta V_t amiloride was then measured in normal (**B**) and CF (**C**) HBECs as indicated. Data shown as mean \pm SEM from n = 16 - 24 HBECs cultured from N = 5 - 8 individual donors. Data were analyzed by ANOVA with Tukey's post-test analyses, * $P < 0.05$, ** $P < 0.01$ and *** $P < 0.001$.

Supplemental Data and Demographic Tables for

SPLUNC1 Degradation by the Cystic Fibrosis Mucosal Environment Drives Airway Surface Liquid Dehydration

Megan J. Webster¹, Boris Reidel¹, Chong D. Tan¹, Arunava Ghosh¹, Neil E. Alexis², Scott H. Donaldson^{1,4}, Mehmet Kesimer¹, Carla M.P. Ribeiro^{1,3} and Robert Tarran^{1,3}

¹Marsico Lung Institute, ²Center for Asthma and Lung Biology, ³Department of Cell Biology & Physiology, ⁴Division of Pulmonary and Critical Care Medicine, The University of North Carolina, Chapel Hill, NC, 27599,

Running Title: SPLUNC1 & CF Sputum

Correspondence to: Robert Tarran
7102 Marsico Hall,
125 Mason Farm Road
University of North Carolina
Chapel Hill, NC, 27599
Email: robert_tarran@med.unc.edu
Contact: 919-966-7052

07.16.18

Supplemental Methods

Proteins and peptides. SPLUNC1 cDNA was kindly provided by Colin Bingle (University of Sheffield, Sheffield, United Kingdom). Recombinant SPLUNC1 protein (rSPLUNC1) was produced using a mammalian expression system and lacked the cleavable N-terminal signal sequence (M1-M19) but was otherwise full length and contained the S18 ENaC inhibitory region (residues G22 through A39)(1). The SPX-101 peptide (aaLPIPLDQTaa) was prepared by the High-Throughput Peptide Synthesis and Array Facility at UNC-Chapel Hill.

Collection of normal and CF sputum samples. Induced and spontaneous sputum samples were obtained as previously described (2, 3). For induced sputum collection, subjects inhaled 3%, 4% and 5% hypertonic saline, each for a 7 min period. To reduce squamous cell contamination, all subjects performed a 3-step cleansing procedure, including (i) rinsing and gargling of the mouth with water, (ii) clearing of the throat, without coughing and (iii) blowing of his/her nose. Following cleansing, induced and spontaneous sputum samples were collected into specimen cups using a cough from the chest. All sputum samples were placed on ice. Samples were incubated in Dulbecco's Phosphate Buffered Saline (DPBS) solution with agitation for 15 min followed by centrifugation and collection of supernatant. Spontaneous sputum collection was similar, except the subjects did not inhale hypertonic saline prior to sputum production. Supernatants were stored at -80°C until required. Donor demographics are shown in supplementary table 1 and 2.

Determination of endogenous NE and SPLUNC1 protein levels in sputum samples. Neat sputum samples were denatured in the presence of 2.5% β -mercaptoethanol at 95°C for ~10 min and were subject to western blot. Samples were transferred to PDVF membranes and blocked using 5% skimmed milk in Tris buffered saline with Tween 20 (TBST-T). For detection of NE protein, membranes were probed using a mouse-monoclonal anti-hELA2 antibody, raised against

residues M1 – N252 (1:3000, R&D systems), primary antibodies were detected using an anti-mouse horseradish peroxidase (HRP) conjugated secondary antibody (Thermo-Fisher Scientific). Membranes were stripped, re-blocked and re-probed for SPLUNC1 using a goat-polyclonal hPLUNC1 antibody raised against residues Q20 – V256 of hPLUNC1 (1:3000, R&D systems), A secondary anti-goat HRP (Thermo-Fisher Scientific) conjugated antibody was used for detection of hPLUNC1. Secondary antibodies were detected by enhanced chemiluminescence.

Degradation of rSPLUNC1. rSPLUNC1 was incubated in combination with normal and CF sputum (pooled from N = 6 donors), NE (Elastin Products Company, #SE563), PBS, and SMM (pooled from N ≥ 3 donors) for specified time periods, at 37°C. Heat-denaturing of sample proteins, in the presence of 2.5% β-mercaptoethanol, at 95°C for ~10 min was performed to stop protease activity. Sputum samples were used neat, except for addition of rSPLUNC1, and SMM samples were diluted 1:2 with PBS. NE was used at indicated concentrations. For matched protein experiments, protein concentrations of pooled sputum (N = 6 normal or CF donors) were determined using the bicinchoninic acid (BCA) assay (Pierce). For inhibition experiments, sputum samples were pooled from N = 6 normal or CF donors and co-incubated with protease inhibitors for one hour prior to addition of rSPLUNC1. Inhibitors used were as follows: EDTA free, protease inhibitor cocktail (PIC, Roche); sivelestat sodium salt (Tocris); aprotinin from bovine lung (Sigma); EDTA (Sigma); E64 (Sigma); CA-074 (Sigma); pepstatin A; leupeptin. Resultant solutions were subject to western blot as described above.

Neutrophil elastase activity assay. NE activity in sputum samples from individual donors was determined using the elastase substrate Suc-Ala-Ala-Ala-MCA (#MAA-3133; Peptides International) at 100 μM. Cathepsin B, K and S/L activity was determined using the substrates Z-Arg-Arg-MCA, Z-Gly-Pro-Arg-MCA and Z-Val-Val-Arg-MCA respectively (Peptides

International). Sputum was diluted 1:1 with assay buffer (final concentrations; 154 mM NaCl; 10 mM HEPES). 10 μ l of sputum buffer mix was added per well in 384-well plates, and 10 μ l of 100 μ M MAA-3133 added to each well. Where specified 20 μ M sivelestat was added to sputum: buffer mix, to give final concentration of 10 μ M. Assays were performed at 37°C using a Tecan infinite M1000 plate-reader, with fluorescence readings taken every 15 minutes. Samples were excited at 380 ± 5 nm and emitted fluorescence collected at 460 ± 10 nm. Resultant AMC concentrations were determined from an AMC standard curve with linear regression analysis. MMP-2/9 activity was determined using a fluorogenic substrate that is cleaved by both MMP-2 and MMP-9 but not by other proteases (DNP-Pro-Leu-Gly-Met-Trp-Ser-Arg; SCP0191, Sigma Aldrich). The MMP-2/9 substrate was incubated with normal and CF sputum for 2.5 h and fluorescence measured kinetically using excitation 280 ± 5 nm and emission 360 ± 10 nm. Sputum protein concentrations were determined using the BCA (Pierce), and fluorescence values adjusted accordingly.

Human bronchial epithelial cell culture (HBECs). Cells were harvested via enzymatic digestion in the presence of antibiotics from human lungs deemed unsuitable for transplantation (non-CF donors) or post-transplantation (CF donors) as per the UNC protocol #03-1396 (4). Freshly isolated (passage zero) or passage one HBECs were seeded on 0.6 cm (24-well hanging inserts, 0.4 μ m pore; Oxyphen, Germany) and were maintained at the air-liquid interface in a modified bronchial epithelial growth medium (5) at 37°C/5% CO₂ in a humidified incubator. Cells were studied 21-28 days following initial seeding.

ASL height measurements and HBEC incubation with sputum. To determine if sivelestat could recover ability of rSPLUNC1 to regulate ASL volume, CF sputum, pooled from N = 6 donors) was incubated ± 30 μ M rSPLUNC1 ± 10 μ M sivelestat overnight at 37°C. For assessment of ability of rSPLUNC1 and SPX-101 to regulate ASL height 30 μ M rSPLUNC1 or

30 μ M SPX-101 were co-incubated with PBS or normal/CF sputum (pooled from N = 6 donors) overnight at 37°C. Prior to experimentation all HBECs were washed apically using PBS. 1mg/ml tetramethylrhodamine dextran (Invitrogen) was added to PBS/sputum and 14 μ l of the resulting solution deposited onto the HBEC mucosal surface. ~30 μ l perfluorocarbon (PFC; FC-77, 3M) was added mucosally. PFC does not displace ASL nor affect ASL height but prevents ASL evaporation (6). Images were acquired using XZ-scanning confocal microscopy (Leica SP5, glycerol 63 x immersion lens) as described previously (7) at a minimum of 10 predetermined points across the entire culture surface using an automated stage 2 hours post sputum addition to HBEC surface.

In some cases, sputum was passed through 10 kDa molecular weight cutoff spin columns (0.5 ml total volume; Millipore-Sigma). Here, sputum was spun in these columns at 13,000 x g for 45 min at 4°C. After this time, the spin column was visually inspected to ensure that all supernatant had passed through. If solution remained in the upper chamber, an additional centrifugation step was performed. The filtrate was then diluted 1:1 with PBS, labeled with rhodamine-dextran and added mucosally to normal HBECs in order to measure ASL height.

Harvesting of airway supernatant of mucopurulent material (SMM). SMM was harvested from the airways of excised human CF lungs as described (8). Harvested material was centrifuged at 10^6 rpm (60 min, 4°C, Beckman TL-100 Tabletop Ultracentrifuge, with a TLA 100.2 rotor), and the supernatant collected. Supernatant was passed through a 0.2 μ m filter and stored at -80°C until required. Donor demographics are shown in supplementary table 3. Endogenous expression of SPLUNC1 in SMM, and degradation of rSPLUNC1 by SMM were determined as described above.

Determination of ENaC and Na⁺/K⁺-ATPase expression in human bronchi. Human lungs unsuitable for transplantation (non-CF donors) or post-transplant (CF donors) were obtained under protocol #03-1396 approved by the UNC at Chapel Hill Biomedical Institutional Review Board. Informed consent was obtained from authorized representatives of all organ donors. Non-CF lungs were from donors with no history of chronic lung disease (supplementary table 4). Bronchi were dissected free from the underlying tissue at 4°C. CF bronchi were selected from relatively disease-free regions. Tissues were rinsed using a lactated Ringers solution and proteins extracted using lysis buffer containing NP40 (4). Donor demographics are shown in supplementary table 4.

Determination of NE mediated cleavage of rSPLUNC1 and SPX-101 by mass spectrometry. 10 µM rSPLUNC1 and 10 µM SPX-101 were incubated with normal or CF sputum (pooled from N = 6 donors) for either 6 or 24 hours. Samples were snap frozen at -80°C prior to processing. Proteomic sample preparation was performed utilizing filter-aided sample preparation (FASP) (9). First, each sample was spin-filtered at 14,000 x g through an Amicon Ultra 4 10 kDa spin filter (Millipore) to collect peptides produced by proteolytic activities under NE, C.F sputum or normal sputum treatment conditions. The remaining material in the filter of higher than 10 kDa molecular weight was reduced in 10 mM dithiothreitol (Sigma-Aldrich) and alkylated in 50 mM iodoacetamide (Sigma-Aldrich). Trypsin digestion (1 ng/µl), was performed in 50 mM ammonium bicarbonate overnight at 37°C. The resulting peptide digests were filtered using the same Amicon Ultra 4 spin filters. Peptide mixes were vacuum-dried and dissolved in 25 µl of 2% acetonitrile and 0.1% trifluoroacetic acid. Five microliter of solubilized peptide material was injected for label-free quantitative proteomic analysis utilizing a Q Exactive (Thermo Scientific) mass spectrometer

coupled to an UltiMate 3000 (Thermo Scientific) nanoHPLC system, and data acquisition was performed as described previously (10).

Proteomic data analysis. The acquired raw data was processed using the Proteome Discoverer 1.4 software (Thermo Scientific) and searched against the UniProt protein database (Homo sapiens, November 2016) and the custom sequence of the SPX-101 peptide using the MASCOT (Matrix Science) search engine with parameters set as follows: 5 ppm mass accuracy for parent ions and 0.02 Da accuracy for fragment ions, with 2 missed cleavages allowed. For the identification of peptides produced by NE activity, cleavage site detection was set to semi-elastase specificity and allowed for variable methionine oxidation and c-terminal amidation, of SPX-101.

For tryptic peptide detection, cleavage specificity was set to semi-tryptic, and Carbamidomethyl modification of cysteines was set to fixed, and methionine oxidation to variable. Scaffold 4.7.5 (Proteome Software Inc.) was used to validate MS/MS-based peptide and protein identifications. Peptide identifications were accepted if they could be established at greater than 95.0% probability by the Scaffold Local FDR algorithm. Protein identifications were accepted if they could be established at greater than 95.0% probability and contained at least 2 identified peptides. Protein probabilities were assigned by the Protein Prophet algorithm (11). Protein quantification was performed by adding the total ion chromatogram intensities of identified peptide ions and fragments assigned to a protein and normalizing the total ion chromatogram to the total intensity of all identified proteins in each sample. The data were normalized via natural log transformations.

Binding of SPLUNC1 and SPX-101 to HBECs. Prior to experimentation HBECs were washed apically using PBS. Cells were loaded with Calcein-AM for 30 minutes prior to apical addition of fluorescently labelled rSPLUNC1 or SPX-101. rSPLUNC1 fluorescently labelled with

amine-reactive Dylight-633 (Thermo Fisher) and 5-TAMRA - SPX-101 were pre-incubated with PBS, normal and CF sputum (pooled from N = 6 donors) for 2 hours and further incubated for 2 hours on the apical surface of normal HBECs. Cells were then washed apically to remove excess, unbound, rSPLUNC1 and SPX-101 and were imaged using a Leica SP8 confocal microscope with a 63x glycerol immersion objective. rSPLUNC1-Dylight 633 nm fluorescence was acquired using a 633 nm laser, and SPX-101 5-TAMRA fluorescence acquired using a 561 nm laser, calcein-AM was imaged sequentially using an argon 488 nm laser.

Transepithelial Potential Difference Studies. A single-barreled transepithelial potential difference (V_t)-sensing microelectrode was positioned in the ASL by micromanipulator and used in conjunction with a macroelectrode in the serosal solution to measure V_t using a voltmeter (World Precision Instruments) as described (12). Perfluorocarbon was present throughout the readings to prevent evaporation of the ASL.

α ENaC-GFP internalisation assay. We have previously shown that SPLUNC1 causes internalisation of α ENaC-GFP and a resulting diminution of GFP fluorescence (13). Here, we used the decrease in α ENaC-GFP as an indicator of SPLUNC1/SPX-101-induced ENaC internalisation. HEK293T cells were seeded onto 10 cm dishes and transiently transfected with 2 μ g each of α ENaC-GFP, β ENaC-untagged and γ ENaC-untagged or GFP alone. 24 hours following transfection, cells were trypsinised and seeded on 96 well culture treated plate (Costar). 30 μ M of rSPLUNC and 30 μ M SPX-101 were incubated overnight \pm 0.1 μ M NE and the reaction stopped by adding 10 μ M sivelestat. Cells were then exposed to either PBS, 30 μ M rSPLUNC \pm 0.1 μ M NE or 30 μ M SPX-101 \pm 0.1 μ M NE in HEK293T cell media (DMEM-HG (4500 mg/l), 10% FBS, 5% Pen-strep) for 1 h at 37°C, and fluorescence measured using a Tecan infinite M1000 plate-reader. Fluorescence was adjusted against that of control, non-transfected, HEK293T cells.

Cells were excited at wavelength 488 ± 5 nm and emission collected at 590 ± 5 nm, with a 5 nm bandwidth.

Statistics. When variances were homogeneously distributed, data were analyzed using ANOVA followed by the Tukey test or Student's t-test as appropriate. When data were not normally distributed, the non-parametric equivalents were used (e.g. Mann-Whitney U-test; Kruskal Wallis Test with Dunn's Multiple Comparisons Test). Data shown are mean \pm SD, or mean \pm SEM as indicated. SPLUNC1 degradation over time curves were fit with single exponentials and analyzed using the Extra Sum of Squares F Test. All data analysis was performed using GraphPad Prism 7.0. Details of experimental numbers are provided in the figure legends. Significance values are denoted as follows; * $P < 0.05$, ** $P < 0.01$, *** $P < 0.001$ and **** $P < 0.0001$. All experiments were performed on a minimum of three separate occasions and are from ≥ 3 donors/group where applicable.

Supplemental Results

SPX-101, but not rSPLUNC1, internalises α ENaC-GFP following exposure to NE. We have previously demonstrated that SPLUNC1 internalises α ENaC-GFP, leading to a decrease in GFP fluorescence, likely as ENaC enters acidic organelles (13). Additionally, we have shown ability of SPX-101, to internalise ENaC subunits (14). Using a multiplate reader, we measured quenching of GFP fluorescence as an indicator of ENaC internalisation (figure S4). We found that SPLUNC1 exposure lead to a quenching of α ENaC-GFP fluorescence in transiently transfected HEK293T cells. Using this approach, we next tested whether NE-exposed rSPLUNC1 was still capable of affecting ENaC. Whilst exposure of HEK293T cells to either 30 μ M rSPLUNC1 or 30 μ M SPX-101 reduced α ENaC-GFP fluorescence, which is indicative of α ENaC-GFP internalization, rSPLUNC1 pre-incubated with NE did not decrease fluorescence (figure S4). However, SPX-101 remained capable of affecting α ENaC-GFP fluorescence even in the presence of NE. In contrast, HEK293T cells transfected with GFP alone, showed no significant change in fluorescence levels following exposure to SPLUNC1 or SPX-101 (figure S4).

Supplemental References

1. Terryah ST, Fellner RC, Ahmad S, Moore PJ, Reidel B, Sesma JI, Kim CS, Garland AL, Scott DW, Sabater JR, et al. Evaluation of a SPLUNC1-derived peptide for the treatment of cystic fibrosis lung disease. *American journal of physiology Lung cellular and molecular physiology*. 2018;314(1):L192-L205.
2. Wu T, Huang J, Moore PJ, Little MS, Walton WG, Fellner RC, Alexis NE, Peter Di Y, Redinbo MR, Tilley SL, et al. Identification of BPIFA1/SPLUNC1 as an epithelium-derived smooth muscle relaxing factor. *Nature communications*. 2017;8(14118).
3. Esther CR, Jr., Peden DB, Alexis NE, and Hernandez ML. Airway purinergic responses in healthy, atopic nonasthmatic, and atopic asthmatic subjects exposed to ozone. *Inhalation toxicology*. 2011;23(6):324-30.
4. Fulcher ML, and Randell SH. Human nasal and tracheo-bronchial respiratory epithelial cell culture. 20131940-6029 (Electronic)).
5. Neuberger T, Burton B, Clark H, and Van Goor F. In: Amaral MD, and Kunzelmann K eds. *Cystic Fibrosis: Diagnosis and Protocols, Volume I: Approaches to Study and Correct CFTR Defects*. Totowa, NJ: Humana Press; 2011:39-54.
6. Tarran R, Grubb BR, Gatzky JT, Davis CW, and Boucher RC. The relative roles of passive surface forces and active ion transport in the modulation of airway surface liquid volume and composition. *J Gen Physiol*. 2001;118(2):223-36.
7. Garland AL, Walton WG, Coakley RD, Tan CD, Gilmore RC, Hobbs CA, Tripathy A, Clunes LA, Bencharit S, Stutts MJ, et al. Molecular basis for pH-dependent mucosal dehydration in cystic fibrosis airways. *Proceedings of the National Academy of Sciences*. 2013;110(40):15973-8.
8. Abdullah LH, Coakley R, Webster MJ, Zhu Y, Tarran R, Radicioni G, Kesimer M, Boucher RC, Davis CW, and Ribeiro CMP. Mucin Production and Hydration Responses to Mucopurulent Materials in Normal vs. CF Airway Epithelia. LID - 10.1164/rccm.201706-1139OC [doi]. 20171535-4970 (Electronic)).
9. Wisniewski JR, Zougman A, Nagaraj N, and Mann M. Universal sample preparation method for proteome analysis. *Nature methods*. 2009;6(5):359-62.
10. Kesimer M, Cullen J, Cao R, Radicioni G, Mathews KG, Seiler G, and Gookin JL. Excess Secretion of Gel-Forming Mucins and Associated Innate Defense Proteins with Defective Mucin Un-Packaging Underpin Gallbladder Mucocele Formation in Dogs. *PLOS ONE*. 2015;10(9):e0138988.
11. Nesvizhskii AI, Keller A, Kolker E, and Aebersold R. A Statistical Model for Identifying Proteins by Tandem Mass Spectrometry. *Analytical Chemistry*. 2003;75(17):4646-58.
12. Tarran R, Trout L, Donaldson SH, and Boucher RC. Soluble mediators, not cilia, determine airway surface liquid volume in normal and cystic fibrosis superficial airway epithelia. *The Journal of general physiology*. 2006;127(5):591-604.
13. Kim CS, Ahmad S, Wu T, Walton WG, Redinbo MR, and Tarran R. SPLUNC1 is an allosteric modulator of the epithelial sodium channel. *The FASEB Journal*. 2018.
14. Scott DW, Walker MP, Sesma J, Wu B, Stuhlmiller TJ, Sabater JR, Abraham WM, Crowder TM, Christensen DJ, and Tarran R. SPX-101 Is a Novel Epithelial Sodium Channel-targeted Therapeutic for Cystic Fibrosis That Restores Mucus Transport. *Am J Respir Crit Care Med*. 2017;196(6):734-44.

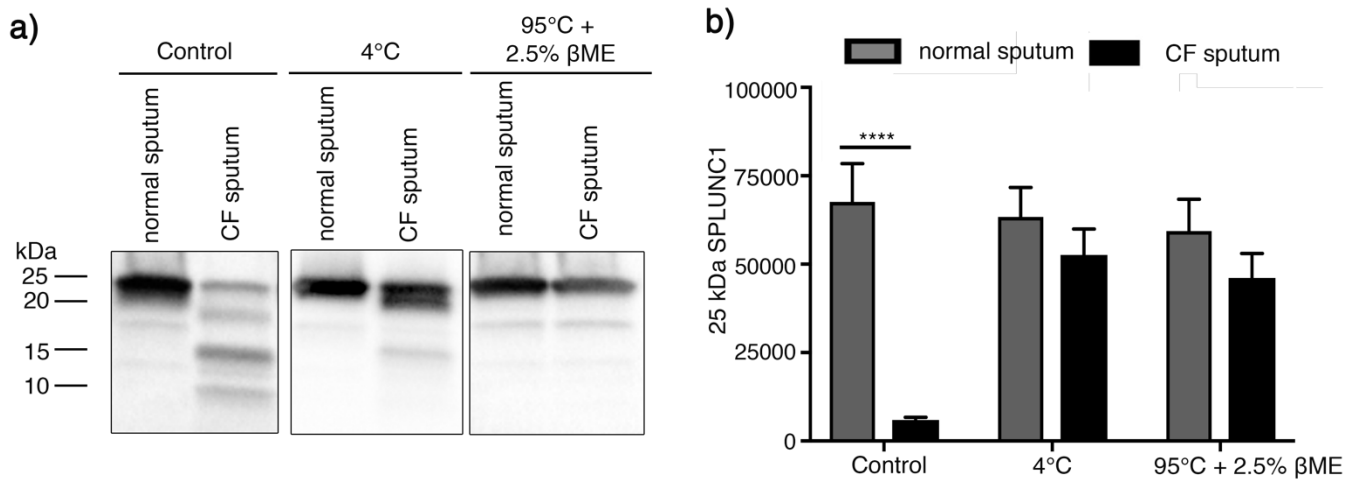


Figure S1 rSPLUNC1 degradation is prevented at 4°C and in the presence of heat denatured CF sputum.

a) Representative Western blots showing rSPLUNC1 incubated at 37°C (control), 4°C and at 95°C with 2.5% β-mercaptoethanol in normal and CF sputum. **b)** Associated densitometry. Data show mean ± SEM from N = 6 individual experiments, **** $P < 0.001$ Two-way ANOVA analysis, with Sidak's multiple comparison test.

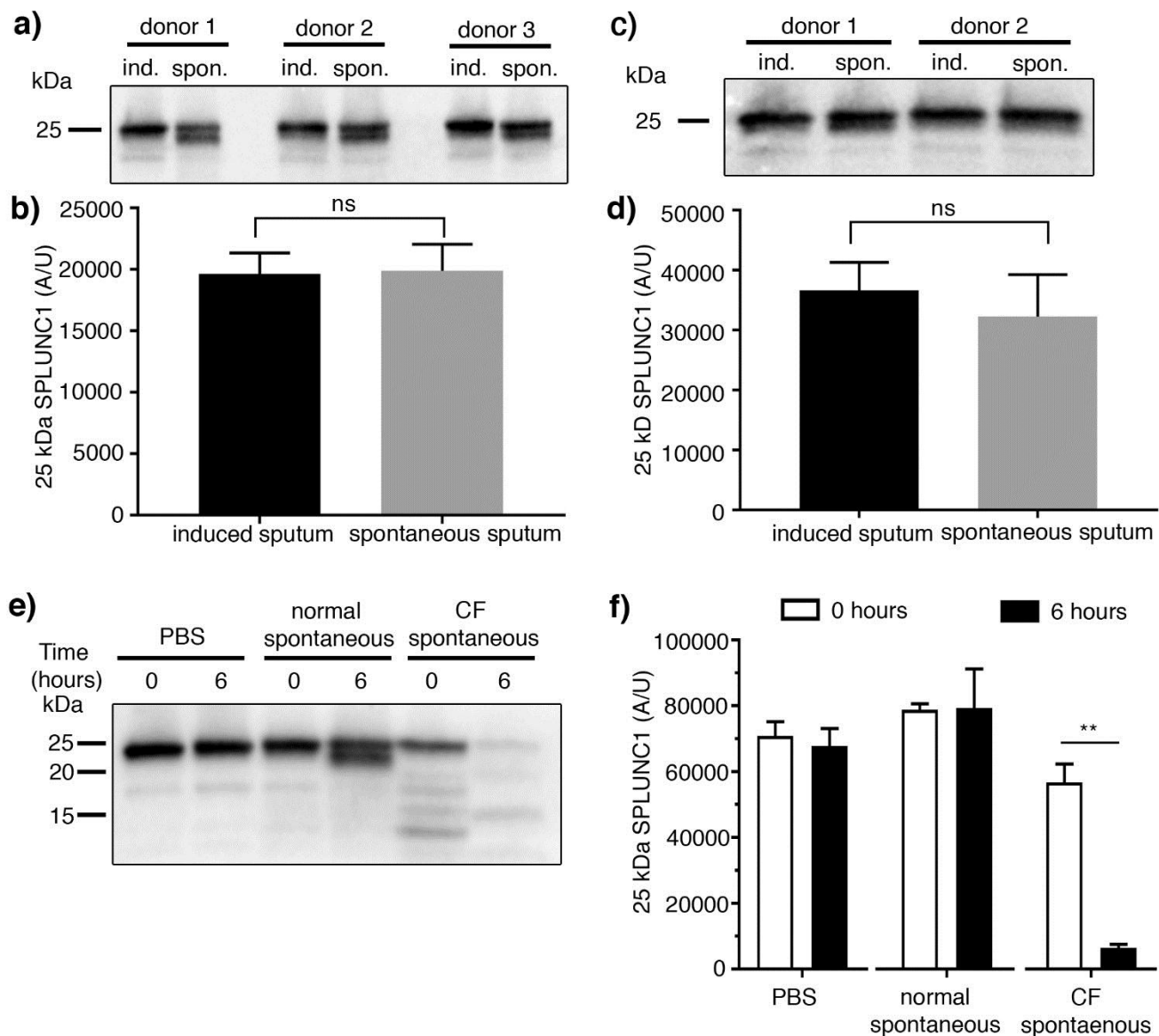


Figure S2. SPLUNC1 is not degraded by normal sputum. **a)** 10 μ M rSPLUNC1 was incubated with 15 μ l of paired normal sputum samples collected spontaneously and via saline induction from N = 3 individual donors and measured by Western blot and **b)** associated densitometry. Data show mean N = 3 \pm SD, Mann-Whitney test analysis. **c)** 10 μ M rSPLUNC1 was incubated with 15 μ g of total protein from paired normal sputum collected spontaneously and via saline induction and **d)** associated densitometry. Data show mean N = 2 donors \pm SD, Mann-Whitney test analysis. **e)** Representative western blot showing relative abundance of SPLUNC1 following incubation of 10 μ M rSPLUNC1 with both normal and CF sputum (pooled from \geq N = 3 donors), collected spontaneously, for 6 h at 37°C and **f)** associated densitometry. Data show mean N = 3 – 6 individual experiments \pm SEM. Mann-Whitney test, t = 0 vs. t = 6 for each respective group. ** $P < 0.001$, CF sputum t = 0 vs. t = 6 h.

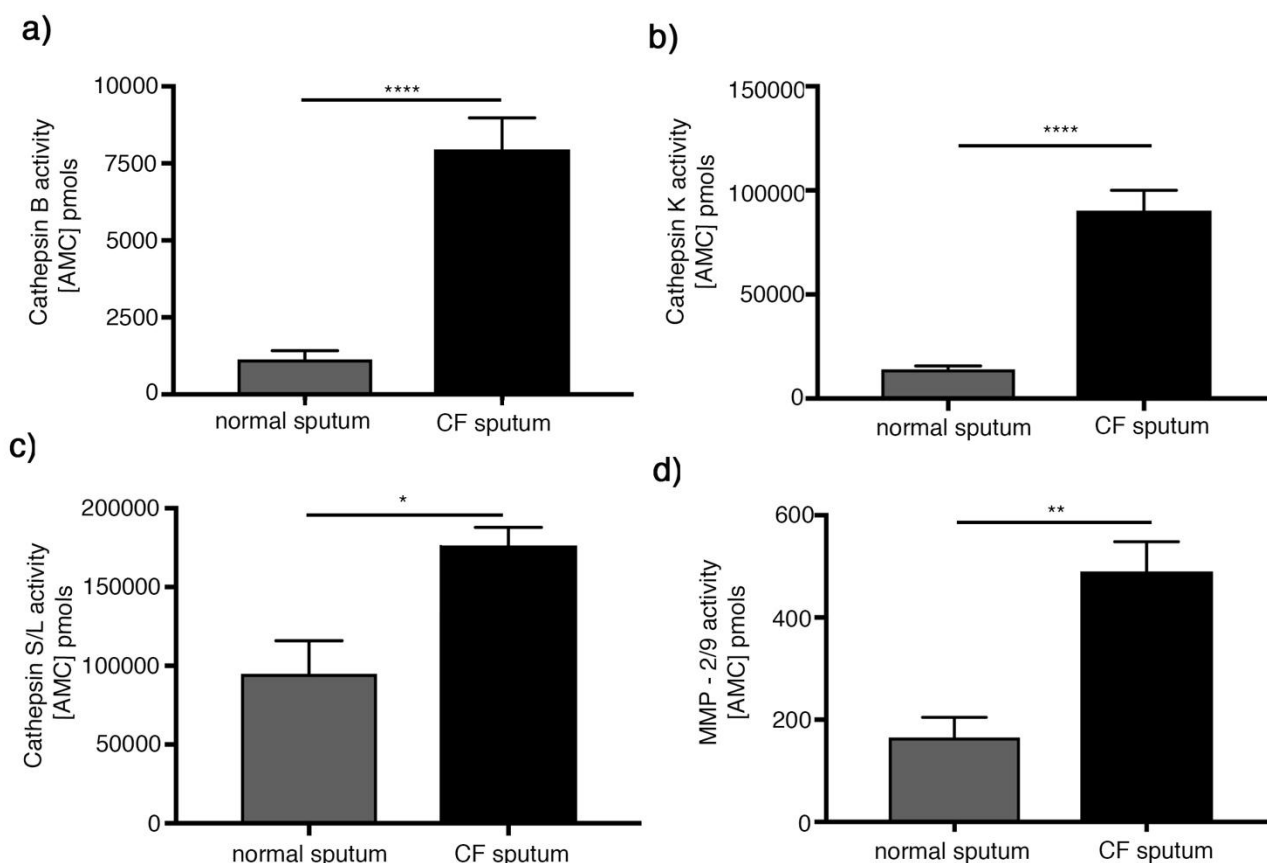


Figure S3. CF sputum cleaves cathepsins B, K, S/L and MMP-2/9 specific substrates. Fluorogenic substrates were incubated with normal and CF sputum over time at 37°C and the subsequent cleavage (i.e. AMC formation) was measured using a multiplate reader. **(a-c)** Show cleavage of 100 μ M of fluorogenic substrates Z-Arg-Arg-vMCA (Cathepsin B), Z-Gly-Pro-Arg-MCA (Cathepsin K) and Z-Val-Val-Arg-MCA (Cathepsins S/L) following 6 h incubation with normal and CF sputum. Fluorescence excitation 380 ± 5 nm, emission 460 ± 10 nm. **d)** Shows the change in fluorescence after incubation of 100 μ M of the fluorogenic substrate DNP-Pro-Leu-Gly-Met-Trp-Ser-Arg in normal and CF sputum for 2.5 h at 37°C. Fluorescence, excitation 280 ± 5 nm and emission 360 ± 10 nm. Data shown as mean \pm SEM; $n = 9$ replicates from $N = 3$ independent experiments using sputum pooled from 6 donors. * $P < 0.05$, ** $P < 0.01$, **** $P < 0.001$ normal vs. CF, Mann-Whitney U test. All data were normalized against total sputum protein concentration.

excited at 380 ± 5 nm and emitted fluorescence collected at 460 ± 10 nm

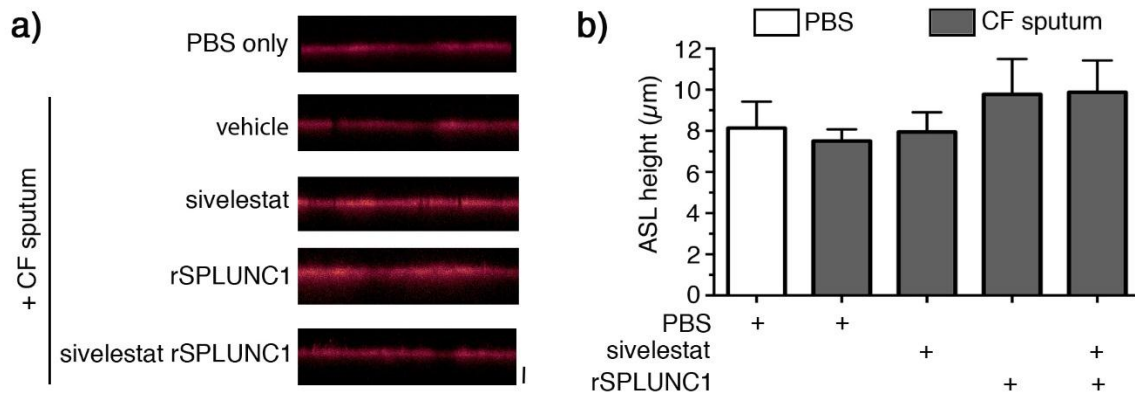


Figure S4. Sivelestat is unable to recover ability of rSPLUNC1 to increase ASL height. **a)** Representative ASL images, following mucosal addition of CF sputum $\pm 30 \mu\text{M}$ rSPLUNC1 and/or $\pm 10 \mu\text{M}$ sivelestat to normal HBECs. **b)** ASL height measurements from $N = 15 - 16$ HBECs per group. Data shown as mean \pm SEM, no significant statistical difference.

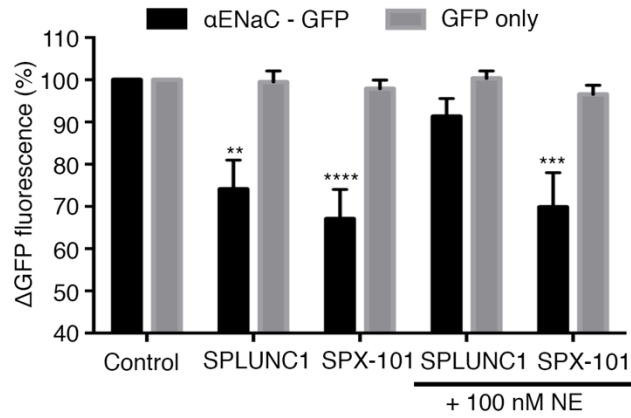


Figure S4. Neutrophil elastase-exposed SPLUNC1 is unable to alter α ENaC-GFP fluorescence in HEK293T cells. HEK293T cells transiently co-transfected with α ENaC-GFP, β ENaC-untagged and γ ENaC-untagged in combination or with GFP alone were incubated with HEK293T cell media \pm 30 μ M rSPLUNC1 or 30 μ M SPX-101, following pre-incubation in the absence and presence of 100 nM NE. GFP fluorescence was determined by plate reader analysis. Data shown mean $n = 16$ -24 wells from $N = 3$ independent experiments \pm SEM. ** $P < 0.01$, *** $P < 0.001$ and **** $P < 0.0001$, Two-way ANOVA with Tukey's post-test analyses. No significant difference was apparent between GFP only fluorescence under any conditions.

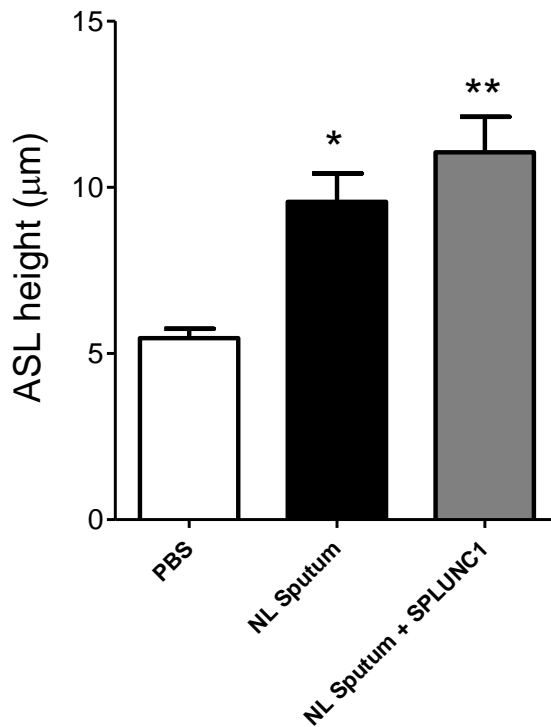


Figure S5. Endogenously-produced normal peptides are bioactive and increase ASL height. Freshly obtained normal sputum from three donors was pooled, centrifuged and filtered using a 10 kDa size exclusion spin column. The filtrate was diluted 1:1 with PBS, labeled with rhodamine-dextran and added mucosally to normal HBECs in order to measure ASL height. Height was measured 6 h after sputum addition and rSPLUNC1 was added at 30 μ M. Data shown as mean \pm SEM. PBS, n = 10; sputum, n=6; sputum + SPLUNC1, n=6. Data from 3 separate experiments. * $P < 0.05$ and ** $P < 0.01$ vs PBS control, by Kruskal-Wallis test with Dunn's multiple comparison.

Supplemental Tables

Table S1: Donor demographics for CF sputum samples. Mean \pm SD ages were 28.3 ± 6.1 and 31.8 ± 10.9 years for normal and CF donors respectively. $P = 0.25$, Student's t-test with Welch's correction.

	Donor	Age at sputum collection	Sex	Ethnicity	FEV1	FVC	Genotype
normal sputum samples	1	25	m	Caucasian	n/a	n/a	n/a
	2	32	f	Caucasian	n/a	n/a	n/a
	3	25	f	Caucasian	n/a	n/a	n/a
	4	33	f	Caucasian	n/a	n/a	n/a
	5	19	f	Caucasian	n/a	n/a	n/a
	6	33	f	mixed	n/a	n/a	n/a
	7	25	m	Caucasian	n/a	n/a	n/a
	8	21	m	Caucasian	n/a	n/a	n/a
	9	19	m	Asian	n/a	n/a	n/a
	10	30	f	Caucasian	n/a	n/a	n/a
	11	34	m	Caucasian	n/a	n/a	n/a
	12	31	f	Caucasian	n/a	n/a	n/a
	13	37	m	African American	n/a	n/a	n/a
	14	21	f	African American	n/a	n/a	n/a
	15	27	m	Hispanic/Latino	n/a	n/a	n/a
	16	40	f	African American	n/a	n/a	n/a
	17	30	f	Caucasian	n/a	n/a	n/a
	18	27	f	Caucasian	n/a	n/a	n/a
CF sputum samples	1	33	m	Caucasian	1.44	3.78	delF508/Q220X
	2	22	f	Caucasian	2.67	3.55	delF508/N1303K
	3	19	f	Caucasian	3.01	3.63	delF508/R347P
	4	28	m	Caucasian	2.66	6.09	delF508/delF508
	5	25	m	Caucasian	2.31	4.31	delF508/R553X
	6	31	m	Caucasian	2.66	4.36	delF508/delF508
	7	27	m	Caucasian	n/a	n/a	delF058/delF508
	8	36	f	Caucasian	1.21	2.28	delF058/delF508
	9	59	m	Caucasian	1.92	2.46	3849+10kbC>T/3659delC
	10	38	m	Caucasian	1.99	2.28	delF058/delF508
	11	20	f	Caucasian	2.89	4.08	delF058/delF508
	12	28	m	African American	1.59	3.38	deltaF508/2184insA
	13	30	f	Caucasian	2.71	3.67	delF058/delF508
	14	32	f	Caucasian	1.74	3.16	delF058/delF508
	15	35	f	Caucasian	1.21	2.28	delF058/delF508
	16	37	m	Caucasian	1.02	2.13	delF058/delF508
	17	18	f	Caucasian	2.61	3.2	deltaF508/R347P
	18	54	f	Caucasian	1.94	1.88	delF058/delF508

Table S2: Donor demographics for induced vs. normal sputum. Mean age was 39.0 ± 18.5 years.

Donor	Age at sputum collection	Sex	Ethnicity	FEV ₁	FVC	Genotype
1	60	f	Caucasian	81%	84%	n/a
2	25	M	Caucasian	80%	87%	n/a
3	32	F	Caucasian	68.5%	178%	n/a

Table S3: Donor demographics for mucopurulent material. Mean age was 27.8 ± 15.6 years

Donor	Age at sputum collection	Sex	Ethnicity	FEV ₁	FVC	Genotype
1	23	f	Caucasian	n/a	n/a	DF/E585X
2	39	f	Caucasian	n/a	n/a	delF058/delF508
3	34	m	unknown	n/a	n/a	delF508/1717-1G>A
4	14	m	unknown	n/a	n/a	delF058/delF508
5	49	f	unknown	n/a	n/a	delF058/delF508
6	8	f	unknown	n/a	n/a	delF508/G330X

Table S3: Donor demographics for normal and CF bronchi. Mean \pm SD ages were 33.0 ± 10.4 and 31.4 ± 9.7 years for normal and CF donors respectively. $P = 0.78$, Student's t-test with Welch's correction.

Donor	Normal/CF	Diagnosis/Genotype	Age	Smoking History	Sex	Ethnicity
1	normal	Head Trauma 2 nd Blunt Injury	26	non-smoker	m	Hispanic
2	normal	Head Trauma 2 nd Blunt Injury	47	non-smoker	f	Caucasian
3	normal	Head Trauma 2 nd Blunt Injury	25	non-smoker	f	Caucasian
4	normal	Head Trauma 2 nd SIGSW	31	non-smoker	m	Caucasian
5	normal	Head Trauma 2 nd Blunt Injury	19	non-smoker	m	Hispanic
6	normal	Head Trauma 2 nd Blunt Injury	40	non-smoker	f	Caucasian
7	normal	Cerebrovascular/Stroke 2 nd ICH	43	non-smoker	m	Caucasian
1	CF	delF058/G85E	22	n/a	m	Caucasian
2	CF	delF058/G542X	25	n/a	f	unknown
3	CF	delF058/delF508	22	n/a	f	unknown
4	CF	delF058/delF508	38	n/a	f	unknown
5	CF	delF058/delF508	48	n/a	m	unknown
6	CF	delF058/unknown	36	n/a	m	Caucasian
7	CF	delF058/delF508	29		m	Caucasian